Conditions for assessing zooplankton abundance with LOPC in coastal waters

B. Espinasse, S. Basedow, L. Berline, S. Schultes, M. Zhou, F Carlotti

Manuscript Details

Manuscript number	PROOCE_2017_45_R2
Title	Conditions for assessing zooplankton abundance with LOPC in coastal waters.
Article type	Full Length Article

Abstract

Recent technical advances in laser-based systems to measure zooplankton distribution have opened new perspectives in ecological and behavioral studies by significantly improving the horizontal and vertical sampling resolution, providing information on zooplankton patchiness and on the influence of small scale physical processes. The application of laser-based systems also led to new challenges on the identification of organisms vs. particulate matter. In areas with high detritus abundances, zooplankton abundances might be overestimated by counting plankton and detritus together. We investigated the contribution of detritus in Laser Optical Plankton Counter (LOPC) data collected during two cruises on the continental shelf of the Gulf of Lion (NW Mediterranean Sea). The study area was characterized by several types of ecoregions owing to the influence of winds, freshwater runoff and intrusion of oligotrophic waters from offshore. We identified the main mechanisms leading to the formation of detritus as a function of environmental conditions and developed a method to assess the contribution of detritus in LOPC counts based on the proportion of large particles (multi-element plankton, MEPs). Highest percentages of detritus (up to 90 % of the counts, mainly particulate organic matter from various sources) were found in stratified conditions associated with relatively high chlorophyll a concentration (chl-a; ca 2 mg m-3). Discontinuities in density profiles alone also resulted in peaks of particles concentrations. We suggested a threshold of 2 % of MEPs in LOPC counts above which the LOPC is most likely counting more detritus than organisms. This easy check of the detritus contribution to total LOPC counts was applied to datasets from different marine ecological situations (glacial input, clear water, productive shelf) and gave successful results in different biogeographical regions (e.g. high latitude and tropical habitats).

Keywords	laser-based sensors; ZooScan; stratification; thin layers; aggregates
Manuscript category	Biological Oceanography

Corresponding Author	Boris Espinasse
Corresponding Author's Institution	University of British Columbia
Order of Authors	Boris Espinasse, Sünnje Basedow, Sabine Schultes, Meng Zhou, Léo Berline, Francois Carlotti

Suggested reviewers	Kohei Matsuno, Pieter Vandromme, Marc Hufnagl, Jason Everett

Submission Files Included in this PDF

File Name [File Type]

cover letter rev.docx [Cover Letter]

Responses LOPC ms_R1.docx [Response to Reviewers]

Highlights.docx [Highlights]

LOPC-ms-R1.docx [Manuscript File]

Fig_LOPC_new.docx [Figure]

Tables.docx [Table]

To view all the submission files, including those not included in the PDF, click on the manuscript title on your EVISE Homepage, then click 'Download zip file'.

Highlights

- A new method to interpret LOPC counts was developed.
- The environmental conditions and the mechanisms resulting in detritus formation were identified.
- LOPC derived indicators were used successfully to determine the contribution of detritus in total counts.
- Thresholds for these LOPC indicators are used to define different situations with varying contribution of detritus.
- The method was applied to worldwide dataset and showed consistent results.

Conditions for assessing zooplankton abundance with LOPC in coastal waters.

Authors:

Espinasse B.[*, 1, 2, 3], Basedow S.[4], Schultes S.[5], Zhou M.[6], Berline L.[1] and Carlotti F.[1]

[1]Aix Marseille Université, CNRS/INSU, IRD, Mediterranean Institute of Oceanography (MIO), UM 110, Marseille, France

[2]Faculty of Biosciences and Aquaculture, Nord University, N-8049 Bodø, Norway

[3]Department of Earth, Ocean, and Atmospheric Sciences, University of British Columbia, 2207 Main Mall, Vancouver, British Columbia, Canada V6T 1Z4

[4]Faculty of Biosciences, Fisheries and Economics, UiT The Arctic University of Norway, N-9037 Tromsø

[5]Aquatic Ecology Group, Ludwig Maximilian University of Munich (LMU), Grosshadernerstr. 2, 82152 Planegg-Martinsried

[6]Shanghai Jiao Tong University, Institute of Oceanology, 800 Dongchuan Rd, Minhang, Shanghai, China, 200240

[*]Corresponding author: bespinasse@eoas.ubc.ca

Abstract

Recent technical advances in laser-based systems to measure zooplankton distribution have opened new perspectives in ecological and behavioral studies by significantly improving the horizontal and vertical sampling resolution, providing information on zooplankton patchiness and on the influence of small scale physical processes. The application of laser-based systems also led to new challenges on the identification of organisms vs. particulate matter. In areas with high detritus abundances, zooplankton abundances might be overestimated by counting plankton and detritus together. We investigated the contribution of detritus in Laser Optical Plankton Counter (LOPC) data collected during two cruises on the continental shelf of the Gulf of Lion (NW Mediterranean Sea). The study area was characterized by several types of ecoregions owing to the influence of winds, freshwater runoff and intrusion of oligotrophic waters from offshore. We identified the main mechanisms leading to the formation of detritus as a function of environmental conditions and developed a method to assess the contribution of detritus in LOPC counts based on the proportion of large particles (multi-element plankton, MEPs). Highest percentages of detritus (up to 90 % of the counts, mainly particulate organic matter from various sources) were found in stratified conditions associated with relatively high chlorophyll *a* concentration (chl-*a*; ca 2 mg m^{-3}). Discontinuities in density profiles alone also resulted in peaks of particles concentrations. We suggested a threshold of 2 % of MEPs in LOPC counts above which the LOPC is most likely counting more detritus than organisms. This easy check of the detritus contribution to total LOPC counts was applied to datasets from different marine ecological situations (glacial input, clear water, productive shelf) and gave successful results in different biogeographical regions (e.g. high latitude and tropical habitats).

Key words: laser-based sensors, ZooScan, stratification, thin layers, aggregates

1. Introduction

Owing to the high variability of physical processes at small scales and their impacts on biological processes, it is necessary to sample plankton at high resolutions for resolving community structure and dynamics. This issue is particularly critical in coastal areas which are the place of nursery and feeding area of many fish, and recent programs such as the MERMEX project (Marine Ecosystems Response in the Mediterranean Experiment; Mermex Group, 2011) called for better evaluation of the pelagic fish habitats in productive coastal areas. Based on optical technologies, several optical sensors have been developed in the recent years for high resolution sampling (Benfield et al*.,* 2007). The in-situ sensors are generally based on imaging technologies with relatively low image resolution (e.g. Video Plankton Recorder, Underwater Video Profiler) or based on the transmission or scattering of a laser beam (e.g. Laser Optical Plankton Counter, Laser In-Situ Scattering and Transmissometry). These optical systems not only provide fine resolution vertical profiles but can also sense fragile particles that are generally destroyed when sampling with a net (González-Quirós and Checkley, 2006). Laboratory sensors are mainly based on the high resolution imaging of samples collected with a net or bottles (e.g. FlowCam, ZooScan). Image-based systems allow for the taxonomic identification of organisms up to a certain degree, while the laser-based systems mainly provide sizes and abundances of the organisms studied. The newly developed holographic technology is an exception, but is more similar to in-situ microscopes facing challenges of sampling volume and data processing (Davies et al*.,* 2011; Talapatra et al., 2013). Laser-based systems measure particles in a wide range of sizes and at high frequency but do not allow to distinguish between organisms and particulate matter. The contribution of detritus to counts can be significant in highly productive regions such as fronts, estuarine systems or upwelling areas, so that the size structure of the plankton community cannot be estimated by abundances derived from in-situ laser-based sensors (Zhang et al*.,* 2000; Ohman et al*.,* 2012; Schultes et al., 2013; Basedow et al., 2014;

Trudnowska et al., 2014). Therefore, in studies focusing on the living part of the spectrum, it is necessary to estimate the proportion of detritus in the total particle pool.

The Laser Optical Plankton Counter (LOPC, Rolls-Royce, England) measures particles and mesozooplankton organisms of sizes between 100 μm and about 3 cm equivalent spherical diameter (ESD) (Herman et al., 2004). It can continuously profile along transects when it is mounted on profiling systems (MVP, profiling float, Acrobats etc., see for example Ohman et al., 2012; Checkley et al., 2008), or can sample vertical profiles when fixed on a net frame or a rosette cage. When particles pass through the tunnel and cross the laser beam, the attenuation of the light intensity is measured by one or several of the 35 photodiode elements, each with 1 mm width. The digital size of a particle is inferred from the intensity changes in shadowed elements, which is converted to ESD. If a particle is recorded by at least 3 diode elements, it will be considered as a multi-element plankton (MEP), in contrast to single element plankton (SEP). In addition to the ESD, more information about the MEPs is provided by the LOPC, allowing to compute an attenuance index (AI). This index has been successfully used to separate detritus and living organisms when targeting large-sized copepods (> 1.5 mm ESD) based on their opacity (Checkley et al., 2008; Gaardsted et al., 2010). For the SEPs, which constitute the dominant part of LOPC counts in the smaller size ranges, no additional information on the transparency of particles is provided, making a direct separation of organisms and detritus impossible. Lately, methods to separate organisms and detritus were proposed, either based on the lognormal distribution expected for size spectra of non-living particles (Petrik et al., 2013; Marcolin et al., 2015) or based on an independent estimation of the size distribution of living organisms from synchronous zooplankton net tows samples (Vandromme et al., 2014).

The proportion of detritus to total LOPC counts varies regionally and seasonally (Schultes and Lopes, 2009; Gaardsted et al., 2010; Ohman et al., 2012; Petrik et al., 2013; Trudnowska et al.,

2014), but the environmental factors influencing this have not been studied in different regions making a general application of thresholds difficult. Here, we use data from winter and spring and from different ecoregions in the Gulf of Lion that are characterized by specific environmental conditions depending on bathymetry, hydrodynamics, atmospheric conditions and freshwater discharge volumes (Espinasse et al., 2014; hereafter E2014; Mermex Group, 2011), to study how environmental conditions influence the LOPC derived indicators AI and %MEPs, and how these reflect the proportion of detritus in LOPC derived abundance. We then apply the thresholds obtained from the Gulf of Lion to a broad range of ecological regions (e.g. polar areas, fjords, open ocean, continental shelf). Our objective is (1) to define the contribution of detritus to particles counted by in-situ laser-based sensors based on environmental parameters and on LOPC derived indicators and (2) to develop thresholds for these indicators to assess the viability of LOPC as a zooplankton counter.

2. Materials and Methods

The study site is the Gulf of Lion, in the northwestern Mediterranean Sea, which has a large continental shelf up to 80 km wide and a mean depth about 100 m. The hydroclimatic conditions in the gulf are characterized by strong northerly winds, high freshwater input mainly from the Rhône River with an annual mean flow of 1721 m^3 s^{-1} (Ludwig et al., 2009) and the Northern Current (also called Liguro-Provencal Current) running along the continental slope. This results in several types of ecoregions characterized by specific environmental conditions (E2014).

Two research cruises were conducted on board the RV Téthys II, one in spring from 25 April to 2 May 2010 (COSTEAU 4) and one in winter from 23 to 27 January 2011 (COSTEAU 6). Each cruise consisted of the same six transects from coast to offshore on the shelf with a total of 135 stations sampled with a CTD Rosette system equipped with a LOPC. At 78 out of these 135

stations, vertical net tows were conducted within 10 to 30 min of the CTD-LOPC casts using a 60-cm diameter Bongo frame equipped with two 120 μm mesh nets. Net samples were used as the reference for zooplankton abundances allowing the estimation of the proportion of detritus in LOPC derived abundance. The LOPC has a flow-through tunnel with an opening of 7 × 7 cm and was integrated with a data logger and a micro-CTD (Applied Microsystems Ltd, Canada). The sampling rate of LOPC was 2 Hz resulting in a vertical resolution of 0.5 m at 1 m s^{-1} lowering speed.

2.1. Environmental conditions

Based on the same cruises, three habitats were defined, characterized by physical parameters such as sea surface salinity, sea surface temperature, bottom potential density, mixed layer depth and stratification index, and biological conditions such as chl-*a* concentration, particle abundances for 3 size classes and the slope of the normalized biomass size spectrum (NBSS) (Table S1, E2014). Habitat #1 was in the near shore area with shallow waters, steep NBSS slope and high chl-*a* concentration; habitat #2 was representative of the zone of dilution of the Rhône plume with stratified waters and flat NBSS slope; and habitat #3 was on the continental shelf with deep mixed layer depth, lowest particle concentrations and intermediate NBSS slope.

2.2. LOPC data processing

Counts and sizes of particles sampled were extracted from the LOPC downcast profiles between 2 m depth below the sea surface and 5 m above the sea bottom. Abundance estimates by the LOPC are dependent on the correct estimation of sampled volume (hereinafter SV). SV can either be estimated from flow speed calculated using the manufacturers equation or estimated based on the depth increment acquired together with LOPC counts. Using the manufacturers equation requires

that enough particles flow through the sampling tunnel. We used the manufactures equation when the number of particles between 150 and 300 µm was > 30 per sample, otherwise SV was estimated as the product of the LOPC opening area by the depth increment. To avoid duplicate counts of particles that can happen in strong wave conditions, LOPC data for which the depth increment was less than 10 cm were removed (5.1 % of the data). All data were processed using an in-house program developed using matlab software (Mathworks, USA). At very high particle densities (>10^6 counts m^{-3}), the data acquisition frequency of the LOPC might not be sufficient. This results first in incoherent M sequences (data stream containing MEP characteristics), and second in the creation of false MEPs due to the coincidence effect of counting at the same time several neighboring particles as one large particle (Schultes and Lopes, 2009; Ohman et al., 2012; Basedow et al., 2014). Incoherent M sequences were observed at 9 out of 135 stations, all of which showed a strong density gradient. If the ratio of MEPs to total LOPC counts (TC) is above 5 % this might indicate coincidence counts (Schultes and Lopes, 2009). We observed ratios above 5 % at 5 out of 135 stations, all located near shore.

2.3. Net sample processing using ZooScan

An aliquot from each net tow sample was processed using the ZooScan (www.zooscan.com) to calculate the vertically integrated abundances and size structure of the zooplankton communities. The net tow sample was split using a Motoda box ensuring a minimum of 1000 particles to be identified by the Zooscan. Each scanned image had a resolution of 2400 dots per inch and was analyzed using ZooProcess (Gorsky et al., 2010), which is embedded in ImageJ, an image analysis software (Rasband, 2005). A total of 46 variables, including geometrical and optical characteristics, are measured by Zooprocess for each individual larger than 300 µm ESD, and are used by the Plankton Identifier software (Gasparini, 2007) to automatically classify the organisms following

the supervised learning algorithms implemented in the TANAGRA free statistical pack (Rakotomalala, 2005). The Random forest algorithm was used for the classification analysis (Breiman, 2001). Two predefined groups were created for the purpose of this study: organisms and detritus. The 'organisms' group was mainly constituted of copepods (Carlotti, Unpublished data); and the 'detritus' group was a composite category composed of phytoplankton aggregates and undetermined fragments of organisms, such as gelatinous parts, molts etc. Most of these detrital particles are created during the net tow by the pressure of the water against the mesh net and by the aggregation of the material inside the cod-end. Therefore, this detritus cannot be related to those counted in situ by the LOPC and was discarded from the ZooScan counts. After the automatic sorting, all images were validated manually.

2.4. Calculation of normalized biomass size spectra

Normalized biomass size spectra (NBSS) were computed from LOPC and ZooScan data. For the ZooScan, the ESD was calculated from the image area of a particle provided by ZooProcess.

For both data, the biovolume was derived from the ESD using the formula:

$$BioV = ESD^3 \times \frac{\pi}{6 \times \sqrt{R}} \quad (1)$$

R, taken equal to 3, is the ratio of the major axis to minor axis of a prolate spheroid and we used an organism density of 1 mg WW mm^{-3} to convert the biovolume into biomass. The NBSS were calculated for each station using the method described in Herman and Harvey (2006). The linear regressions were fitted to the part of a spectrum in the size range starting from the mode of the spectrum in the small size and ending at the first empty size class.

2.5. LOPC derived indicators

We investigated two potential indicators that might reflect the proportion of detritus in LOPC counts: (1) the proportion of MEPs in the total number of counts (%MEPs) and (2) the AI indicating the transparency of particles. The theoretical size threshold between SEP and MEP is about 1.5 mm (Herman et al., 2004), but MEPs generally have a small ESD relatively to their maximum length because they do not attenuate much light. We hypothesize that, in a region where most of the organisms are below 1.5 mm of ESD (about 2.5 mm length for a copepod), the MEPs are mainly composed of detritus so that the %MEPs mainly varies as a function of detritus concentration.

The attenuance index (AI) was calculated based on Checkley et al. (2008) and updated by Basedow et al. (2013),

$$AI = \sum_{i=2}^{n-1} DS_i \frac{1}{((n-1)-1) \times maxDS} \quad (2)$$

where DS is the digital size of the MEP for each photodiode element, n the number of elements and maxDS is the maximum digital size of a MEP (corresponding to a complete occlusion of a diode element). Based on the definition, AI varies from 0 for very transparent particles to 1 for very opaque particles. The DS values of the elements at the edges of the MEP sequence were not included to compute the AI, because these elements may only partly cover the area of a diode, resulting in a lower AI than real (Basedow et al., 2013). The AI should not be understood as an opacity index only, because both opacity and shape of a particle contribute to it. For example, a filamentous diatom (opaque but with lots of empty space) and an appendicularian (a very transparent organism) could have a similar ESD and AI because they would attenuate the same quantity of light, but they could have very different biovolume and opacity characteristics.

2.6. Estimation of the detritus part in LOPC counts

In the ocean, particulate matter consists of various types of particles including detrital aggregates, decaying fragments of organisms, fecal pellets and sediments (Alldredge and Silver, 1988), which will be called detritus hereafter. A total of 78 quasi-synchronous LOPC casts and net tows was analyzed. Because the reliability and accuracy of abundance assessment with the ZooScan is very high, the estimated abundance in the group 'organisms' was used as reference for zooplankton abundance in this study. Nevertheless, it is important to keep in mind that nets are biased estimators of the in-situ abundance of organisms that undersample fragile organisms and are limited to a certain size range. Also, net avoidance by mobile organism and net clogging can bias abundance estimates, but were unlikely to be an issue in our study. The size of copepods in the Mediterranean Sea is generally small and the largest individuals of the dominant taxa *Paracalanus* and *Clausocalanus* are about 1 mm length at the adult stage (Gaudy et al., 2003) limiting their escaping capability. Moderate chl-*a* concentrations (maximum of 2.75 mg m^{-3}) measured during the cruises prevented the net from clogging (mesh size 120 µm).

The size range of zooplankton captured quantitatively is limited by the mesh size for the net samples and the volume filtered for the LOPC (Vandromme et al., 2012). Based on the NBSS, we estimated that the valid overlap in size range with correct estimation of abundance from both the ZooScan and LOPC was from 350 µm to 2000 µm ESD.

We hypothesize as Vandromme et al. (2014) that within this size range the difference between the ZooScan and LOPC is due to particulate matter counted in addition to zooplankton by the LOPC. For size fraction i=350 to 2000 µm, the percentage of detritus in LOPC abundances was calculated following the equation:

$$\%\ \text{detritus}_i = (\text{LOPC\_ab}_i - \text{ZooScan\_ab}_i) / \text{LOPC\_ab}_i \quad (3)$$

ZooScan abundances were higher than LOPC abundances at 14 stations out of 78, albeit only slightly for 11 of them (< 30%), the stations being distributed over the gulf without any detectable

pattern. These stations were not included in the statistical analysis. The factors potentially leading to this situation and the implications for this study are discussed later.

2.7. Statistical analyses

The Kruskal-Wallis test (one way ANOVA on ranks) was performed to identify potential links between the percentage of detritus and LOPC particle characteristics (AI and %MEPs) on one hand, and between percentage of detritus and the zooplankton habitats representative of different environmental conditions on the other hand. This test was chosen because of the non-normal distribution of the variables. Post-hoc tests were performed to assess the differences between habitats. All statistical tests were performed using the R statistical software (version 3.2.3, R Development Core Team, 2016), Kruskal-Wallis using kruskal.test and and post-hoc tests, posthoc.kruskal.nemenyi.test (package PCMCR, version 2016-01-06).

3. Results

3.1. *Spatiotemporal distribution of particle characteristics and detritus*

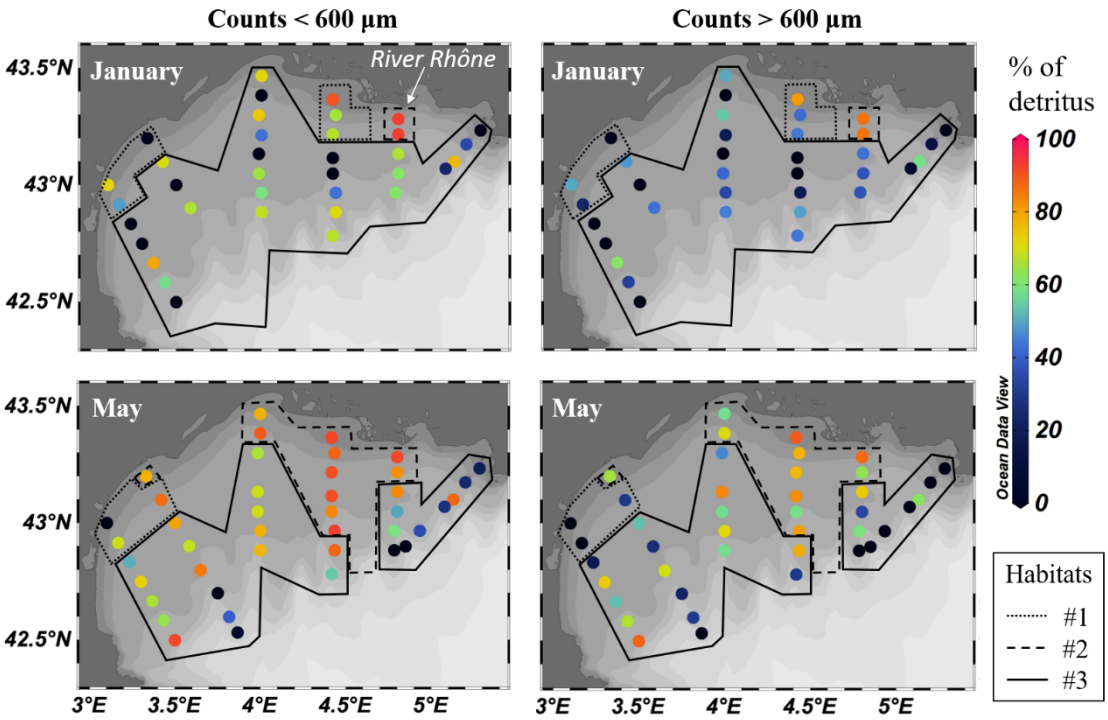

Fig. 1. Percentage of detritus in LOPC counts in January 2011 (top) and May 2010 (bottom) in the Gulf of Lion for two particle size fractions: below (left) and above (right) 600 µm size. The three habitats defined in Espinasse et al. 2014 are delineated, habitat #1: near shore area; habitat #2: area affected by the Rhône waters; habitat #3: continental shelf.

The variability of the detritus in terms of spatial and temporal distribution was analyzed for two size fractions, above and below 600 µm ESD (corresponding roughly to a total length of 1 mm for a copepod) (Fig. 1). For both seasons, the percentage of detritus in LOPC counts was lower for the larger size fraction than for the smaller one while their spatial patterns were similar. In winter, the percentage of detritus of both small and large size was relatively low (mainly under 50%), except

for the three stations closest to the Rhône mouth. In spring, detritus represented a large part of the LOPC counts (mainly over 50%) in the entire continental shelf. Only at the easternmost transect,

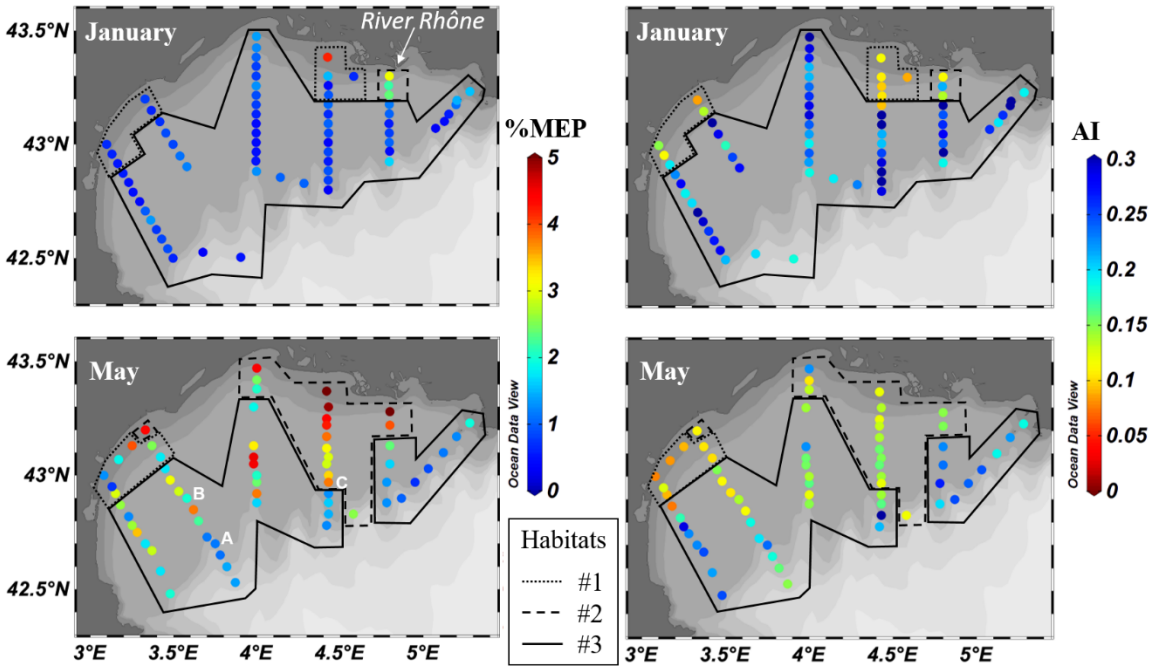

influenced by offshore water, a lower percentage of detritus was observed.

Fig. 2. Indicators of particles counted by the LOPC in January 2011 (top) and May 2010 (bottom) in the Gulf of Lion: % of MEPs in total LOPC counts (left side) and the MEPs' mean attenuance index (AI, right side). The three habitats defined in Espinasse et al. 2014 are delineated, habitat #1: near shore area; habitat #2: area affected by the Rhône waters; habitat #3: continental shelf. The three representative stations (A, B and C) shown in Fig. 4 are marked in the lower left panel.

Throughout the study area, spatiotemporal differences in LOPC particle counts and characteristics were observed (Fig. 2). In spring, higher values (> 2%) of the percentage of MEPs in total LOPC counts were generally observed compared to winter (< 1%). However, high values were observed in front of the Rhône mouth in winter and low values beyond the continental slope in spring. The AI of the MEPs showed a pattern rather similar to the %MEPs (Fig.2, right panels). Some differences existed, such as low values for the near shore area in the western part of the gulf in

winter and high values for some stations in the most western transect in spring. A highly significant correlation was found between the percentage of detritus and the %MEPs (r^2=0.54, p <10^{-9}) strongly supporting our hypothesis that the %MEPs can be used as an indicator of detritus (Fig. 3).

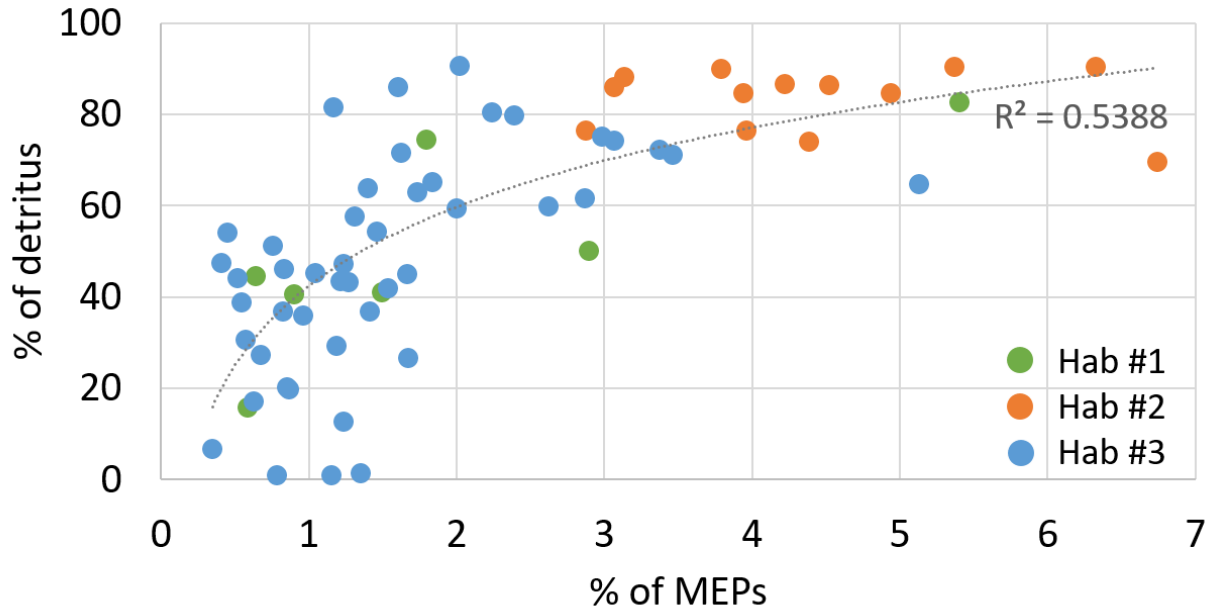

Fig. 3. Percentage of detritus in LOPC counts relative to the percentage of MEPs in total LOPC counts. The data were fitted with a logarithmic function. Habitats as defined in Fig. 1 and 2.

3.2. Statistical relationships between environmental conditions and LOPC indicators

Station details including LOPC and ZooScan abundances (# part. m^{-3}), percentage of detritus in LOPC counts, percentage of MEPs in LOPC counts, mean AI, slope of the NBSS, water column stratification index, maximum of chl-*a* concentration (mg m^{-3}) and sampling depth. Considering the station denotation, the letter specifies the transect, from west (A) to east (F), and the number the position of the station along the transect from coast (1) to offshore (6-8). For example, A1 is the furthest west station and E1 is located in front of the mouth of the River Rhône. The stations A, B and C displayed in Figs 4-5 are indicated. No stratification is stated as n.a. for non-applicable. When ZooScan counts were higher than LOPC counts and, therefore, the percentage of detritus cannot be computed, x states for < 30 % difference in count and X > 30%.

Cruise	Station/ Habitat	LOPC Ab.	ZooScan Ab.	% of det.	%MEPs	AI	Slope	Strat. ind.	Max. chl-*a*	Depth

COSTEAU 6	A1/1	6514	3609	45	0.63	0.15	-1.07	n.a.	0.93	25
Jan 2011	A2/1	5427	4567	16	0.53	0.19	-0.96	n.a.	0.88	35
	A3/3	4533	5900	x	0.44	0.28	-0.87	n.a.	0.77	60
	A4/3	1955	3539	X	0.39	0.20	-0.99	n.a.	0.56	80
	A5/3	4370	1525	65	1.31	0.30	-0.73	n.a.	0.60	90
	A6/3	2426	1555	36	0.80	0.27	-0.81	n.a.	0.67	100
	A7/3	1815	1850	x	0.62	0.21	-0.94	n.a.	0.66	170
	B1/1	7111	21250	X	0.76	0.09	-1.30	n.a.	1.28	20
	B2/3	4046	1975	51	0.67	0.32	-0.79	n.a.	1.14	45
	B3/3	3005	3569	x	0.81	0.17	-0.93	0.03	0.97	80
	B4/3	3270	1853	43	1.19	0.28	-0.77	n.a.	0.82	90
	C1/3	9845	3567	64	1.37	0.39	-0.61	n.a.	0.83	20
	C2/3	6300	6985	x	1.00	0.27	-0.78	n.a.	0.92	45
	C3/3	2535	1364	46	0.78	0.21	-0.81	n.a.	0.52	75
	C4/3	3537	2500	29	0.89	0.26	-0.81	n.a.	0.77	80
	C5/3	2524	2903	x	0.62	0.29	-0.83	n.a.	0.70	85
	C6/3	2875	1605	44	0.47	0.22	-0.91	n.a.	0.63	90
	C7/3	1508	1048	31	0.45	0.24	-0.91	0.02	0.75	90
	C8/3	3856	2244	42	1.27	0.18	-0.86	n.a.	0.65	130
	D1/1	36498	6313	83	4.18	0.11	-0.77	0.67	1.40	17
	D2/1	4318	2543	41	1.49	0.11	-0.99	0.14	1.05	40
	D3/1	3209	1907	41	0.90	0.10	-1.14	0.25	0.99	65
	D4/3	2388	1979	17	0.63	0.42	-0.73	0.13	0.79	75
	D5/3	2834	3263	x	0.82	0.21	-0.88	n.a.	0.67	90
	D6/3	1548	1237	20	0.82	0.25	-0.79	n.a.	0.90	110
	D7/3	1756	803	54	0.89	0.31	-0.74	n.a.	0.45	270
	D8/3	453	238	48	0.33	0.29	-0.82	n.a.	0.46	200
	E1/2	10710	1500	86	3.06	0.11	-0.82	0.84	0.75	50
	E2/2	7154	965	87	2.35	0.14	-0.80	1.21	0.60	85
	E3/3	3065	1681	45	1.02	0.24	-0.80	0.20	0.74	95
	E4/3	2367	1495	37	0.80	0.28	-0.82	n.a.	0.71	100
	E5/3	992	608	39	0.43	0.32	-0.89	n.a.	0.53	300
	F1/3	3768	5250	x	1.56	0.19	-0.85	n.a.	0.71	55
	F2/3	2239	1641	27	1.11	0.38	-0.68	n.a.	0.70	80
	F3/3	1767	813	54	0.40	0.20	-0.84	n.a.	0.68	100
	F4/3	1257	1174	7	0.33	0.26	-0.95	n.a.	0.70	130
COSTEAU 4	A1/1	5924	9851	X	1.29	0.08	-1.02	0.06	1.70	25
May 2010	A2/1	15354	7646	50	2.90	0.09	-1.03	0.11	2.43	36
	A3/3	5343	3021	43	1.22	0.17	-0.89	0.05	0.87	55
	A4/3	4733	1361	71	3.46	0.23	-0.64	0.03	0.58	80
	A5/3	4168	1599	62	2.82	0.25	-0.66	0.03	0.63	80
	A6/3	3946	1462	63	1.73	0.22	-0.82	0.04	0.46	100
	A7/3	3088	287	91	2.00	0.25	-0.71	0.03	0.50	145
	B1/2	19440	5070	74	4.37	0.11	-0.79	0.29	0.33	20
	B2/1	10675	2725	74	1.78	0.10	-0.99	0.18	1.68	50
	B3/3	7298	1887	74	3.06	0.11	-0.87	0.20	0.73	80
Stn. B	B4/3	3933	1597	59	2.00	0.14	-0.78	0.17	0.53	90

	B5/3	2373	462	81	2.24	0.18	-0.74	0.11	0.82	150
Stn. A	B6/3	1687	1736	x	1.15	0.24	-0.80	0.04	1.10	200
	B7/3	2271	1433	37	1.41	0.16	-0.90	0.15	0.55	265
	B8/3	1411	1392	1	1.35	0.15	-0.92	0.10	0.76	200
	C1/2	44544	13513	70	4.44	0.22	-0.62	0.47	0.43	20
	C2/2	10514	1622	85	2.07	0.13	-0.87	0.28	1.35	45
	C3/3	5109	2046	60	1.89	0.14	-0.85	0.23	0.80	75
	C5/3	8609	2382	72	3.24	0.22	-0.65	0.25	0.90	90
	C6/3	8902	3134	65	4.50	0.15	-0.75	0.27	0.61	90
	C7/3	5193	1294	75	2.43	0.16	-0.76	0.36	0.91	85
	C8/3	3491	993	72	1.62	0.15	-0.85	0.24	0.41	140
	D1/2	33804	3244	90	5.87	0.12	-0.68	0.61	0.77	15
	D2/2	21171	3231	85	4.93	0.14	-0.62	0.41	0.69	40
	D3/2	16739	2239	87	4.22	0.13	-0.72	0.54	0.90	65
	D4/2	15823	1856	88	3.13	0.15	-0.71	0.74	1.20	75
	D5/2	11200	2645	76	2.87	0.16	-0.66	1.05	1.13	95
Stn. C	D6/2	8968	905	90	3.79	0.12	-0.68	0.51	2.27	115
	D7/3	4356	613	86	1.58	0.16	-0.89	0.40	0.49	200
	D8/3	1257	664	47	1.23	0.21	-0.79	0.25	0.59	200
	E1/2	40713	3925	90	5.21	0.15	-0.60	2.10	2.73	50
	E2/2	15312	3602	76	3.97	0.15	-0.72	0.71	2.70	90
	E3/3	10570	2130	80	2.38	0.23	-0.74	0.31	0.44	95
	E4/3	2734	1503	45	1.65	0.24	-0.74	0.07	0.54	100
	E5/3	2047	869	58	1.31	0.27	-0.76	0.06	0.49	200
	E6/3	2284	2922	x	1.29	0.20	-0.82	0.05	1.35	200
	F1/3	4991	5357	x	1.96	0.19	-0.79	0.02	0.73	60
	F2/3	2679	2340	13	1.22	0.22	-0.78	0.05	0.45	80
	F3/3	4086	755	82	1.15	0.19	-0.83	0.07	0.40	100
	F4/3	1816	1455	20	0.86	0.24	-0.83	0.03	0.54	200
	F5/3	1799	1307	27	0.67	0.24	-0.90	0.01	0.76	200
	F6/3	1645	2046	x	1.01	0.25	-0.83	0.02	0.55	200

To get a better understanding of the mechanisms underlying the relationship between the %MEPs and the detritus abundances, we tracked how they changed with different environmental conditions (Table 1) as described by the three habitats defined in E2014. The percentage of detritus, percentage of MEPs and AI changed significantly between the habitats defined in E2014 (Table 2). The area affected by the Rhône River freshwater (defined as habitat #2) had a significantly higher percentage of detritus and a higher %MEPs than the other two habitats. The average %MEPs in habitat #2 was 2.48 (2.18-3.07, $n = 3$) in January and 3.51 (2.07-5.88, $n = 17$) in May compared to an overall

average of 1.65 (0.67-4.59, *n = 48*) and 0.67 (0.32-4.18, *n = 67*) for habitats #1 and #3. The continental shelf (habitat #3) was characterized by particles with a significantly higher AI, overall average of 0.23 (0.09-0.43, n = 97), than for habitats #1 and #2, overall average of 0.11 (0.07-0.19, n = 18) and 0.14 (0.10 – 0.22, n = 20), respectively. The changes in distribution of detritus, %MEPs and AI within the habitats showed that the conditions where stratified waters were coupled with high chl-*a* concentrations in the surface layer resulted in a higher percentage of detritus and a higher %MEPs. This was observed in habitat #2 influenced by Rhône waters. The lower AI and higher percentage of detritus in habitat #2 demonstrated the general transparency of the detritus, compared to the higher AI associated with lower detritus observed on the continental shelf (habitat #3).

Table 2. Kruskal-Wallis test applied on the percentage of detritus, % of MEPs and AI considering as factors the 3 habitats defined in Espinasse et al. 2014. Post-hoc results are also shown.

Parameter	X^2	p-value	Post-hoc			
%detritus	25.88	$2.39\ 10^{-6}$		Habitat #1	Habitat #2	H2 > H1;
			Habitat #2	<0.001	-	H2 > H3
			Habitat #3	n.s.	<0.001	
%MEPs	39.09	$3.23\ 10^{-9}$		Habitat #1	Habitat #2	H2 > H1;
			Habitat #2	<0.001	-	H2 > H3
			Habitat #3	n.s.	<0.001	
AI	61.85	$3.7\ 10^{-14}$		Habitat #1	Habitat #2	H3 > H1;
			Habitat #2	n.s.	-	H3 > H2
			Habitat #3	<0.001	<0.001	

3.3. Detailed analyses of particle characteristics at three typical stations

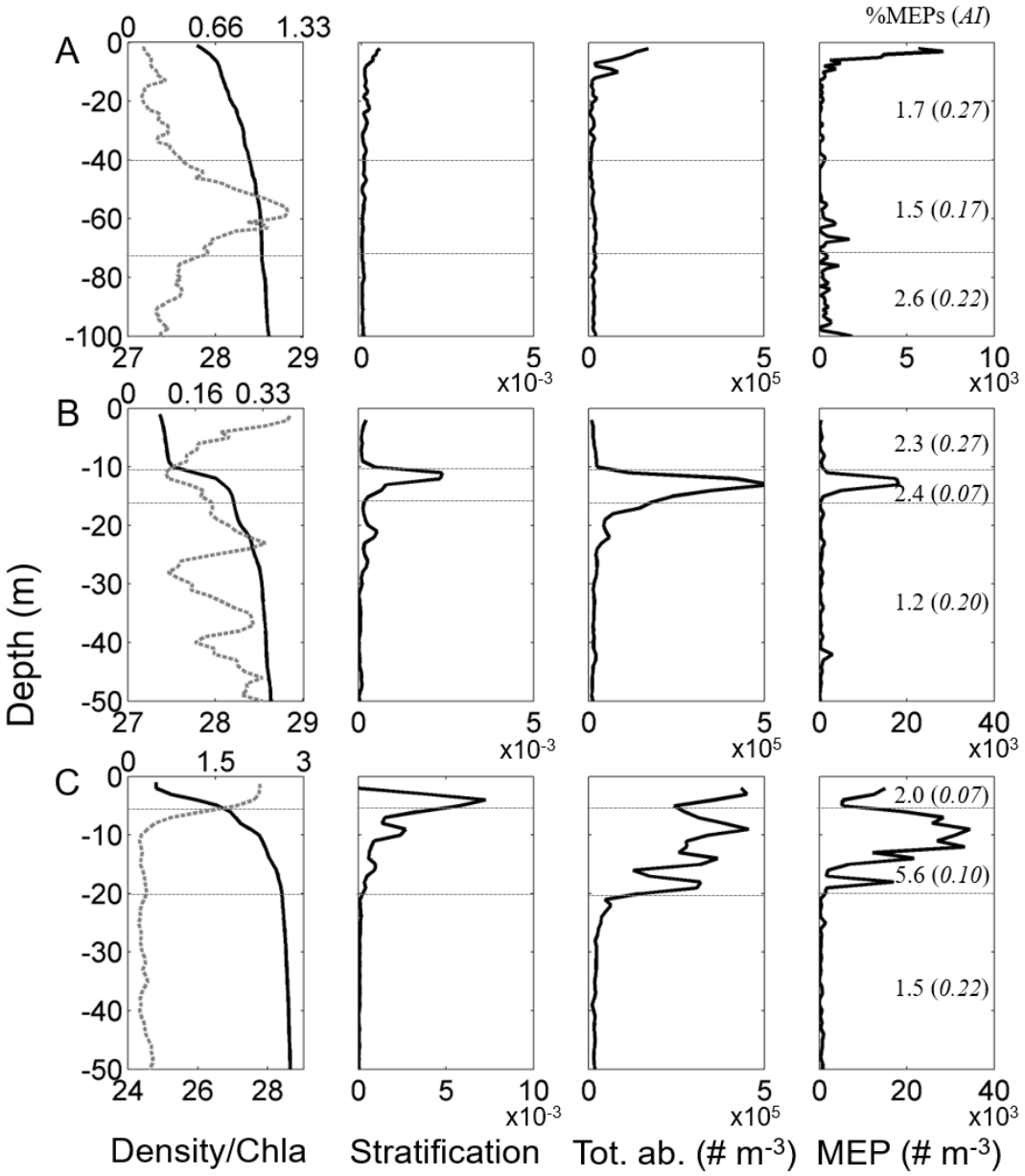

Fig. 4. Vertical profiles of water density σ_θ (kg m^{-3}; full line, left panels) and chl-*a* concentration (mg m^{-3}; dashed grey line, left panels), the stratification (Brunt-Väisälä frequency squared N^2, s^{-2} ; center left panels), total LOPC abundance (Tot. ab., centre right panels) and MEP abundance (right panels) at stations A, B and C typical of different environmental conditions. The integrated % of MEPs and the average of AI are specified in brackets for two (station A) or three (stations B and

C) depth layers (horizontal dotted grey lines). The location of the stations is shown in Fig. 2. Note the change in x-axis range among stations.

Based on the results provided by the spatial distributions, three stations representing different scenarios in terms of water stratification and chl-*a* concentration were chosen to investigate the vertical variations of TC, MEPs, %MEPs and AI (Fig. 4).

Vertical profiles at station A showed a homogeneous water density and Brunt-Väisälä frequency, and a deep peak of chl-*a* concentration reaching 1.2 mg chl-*a* m^{-3} at 60 m depth. TC and MEP counts had a peak in the surface layer, reached minima between 20 and 40 m, and slightly increased in the layer between 40 and 70 m and the layer below, while AI was lower in the layer of maximum of chl-*a*. At this station, %MEPs and average AI integrated over the entire water column were 1.15 and 0.24, respectively, and the percentage of detritus was estimated to be of 0% (i.e. LOPC abundance = ZooScan abundance).

Profiles at station B showed a stratified water column with a pycnocline located at 12 m depth and relatively low chl-*a* concentration (0.09-0.36 mg chl-*a* m^{-3}). TC and MEP counts peaked in the pycnocline layer. The AI was high in the surface layer (0.27) and dropped strongly in the pycnocline layer to 0.07. %MEPs was relatively high in the surface layer and increased below the pycnocline. At this station, %MEPs and average AI integrated over the entire water column were 2.00 and 0.14, respectively, and the percentage of detritus was estimated to be of 59% in LOPC counts.

Station C was located in the Rhône plume, approximately at 45 km from the Rhône mouth, showing a thin layer of very low salinity water in surface resulting in strong stratification. Highest chl-*a* concentrations were found in the surface layer (maximum of 2.3 mg chl-*a* m^{-3}). The halocline layer between surface low salinity water and deep saltier water was spread between 5 and 20 m depth. High LOPC abundance and very high MEP abundance were found in the surface and gradient

layers. Very low AI values were observed in the surface layer, and low AI values and very high values of %MEPs were found in the halocline. Below the stratified layer these parameters were similar to those at stations A and B. At station C, %MEPs and average AI integrated over the entire water column were 3.79 and 0.12, respectively, and the percentage of detritus was estimated to be up to 90% in LOPC abundance (i.e. LOPC abundance was 10 times the zooplankton abundance estimated with the ZooScan).

The NBSSs of particles estimated for the whole water column by both devices showed good agreement in their size range overlap (1.1 to 3.4 log(µg)) for the stations A and B (Fig. 5), but relatively high difference for the station C with higher biomasses from LOPC. NBSS inside the different water layers provides information on the homogeneity of the biomass distribution as a function of depth. The NBSSs at station A were vertically homogeneous, although the biomass in the surface layer was slightly higher. The NBSSs at station B and C showed much higher values in the stratified layers. At station C, the NBSS in the surface layer was characterized by high biomass values in the lower size classes and a relatively steep NBSS slope (-1.21) towards higher size classes, which is a signature of productive layer. In the halocline and below, the NBSS slopes were flatter (-0.64 and -0.79) and similar in shape, potentially resulting from a uniform distribution of the detritus along the size spectrum.

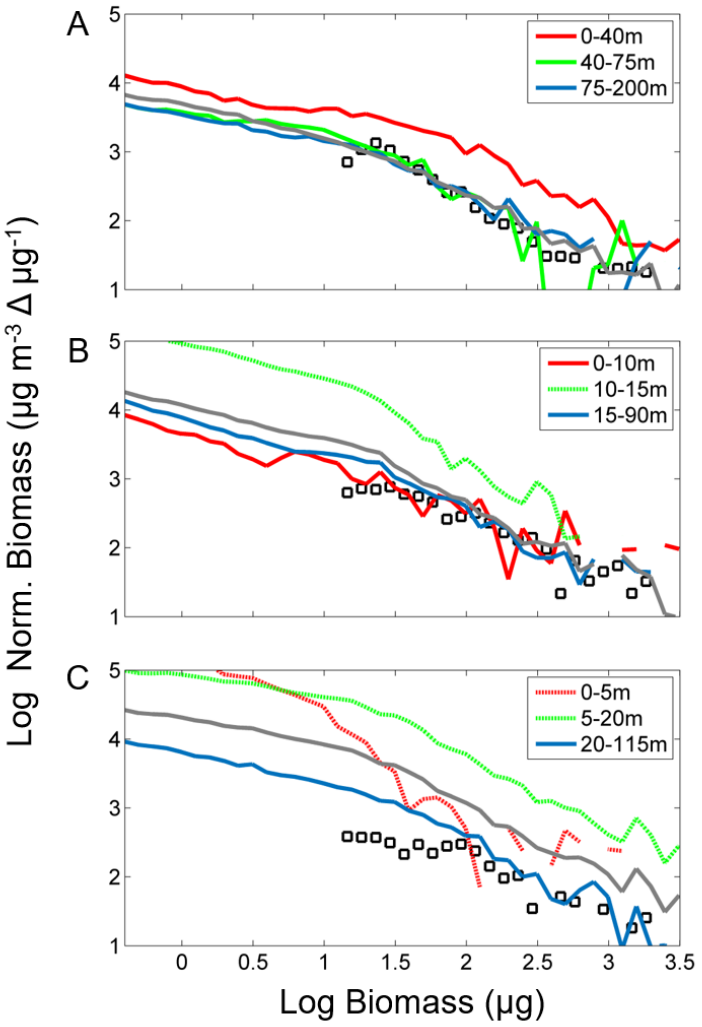

Fig. 5. Normalized biomass size spectra (NBSS) from LOPC data integrated over the water column (grey line) and in different layers as defined in Fig. 4 (blue lines, NBSSs in stratified layers are displayed with dashed line), and NBSS from ZooScan data over the whole water column (black squares) for 3 stations typical of different environmental conditions (see Fig. 2 and 4).

3.4. Typical distribution of particles and LOPC indicators under specific environmental conditions

Four typical associations between particle distribution and environment could be identified from the detailed analyses of the stations:

(1) Vertical density stratification coincided with a peak in LOPC counts. To test this statement, we investigated the occurrences of a peak of LOPC abundance in relation to the occurrences of a strongly stratified layer at all stations. A peak of LOPC counts was defined for concentrations > 50 % of the average concentration over the whole profile. Stratified layers were defined using a threshold value of $N^2 = 0.001\ s^{-2}$ (Brunt-Väisälä frequency). A co-occurrence between a stratification layer and a peak of LOPC counts was found for 93 % of the stations (81 out of 87 stratified stations, χ^2 test, $p < 10^{-9}$).

(2) The percentage of MEPs in total LOPC counts increased when stratification was associated with high chl-*a* concentrations (chl-*a* > 1 mg m^{-3}) in the surface layer. Density gradients in the water column typically lead to aggregate formation, and the number of aggregates increase with high production in the surface layer resulting in more MEPs, which is illustrated in the MEP profile and NBSS comparison at station C (Fig. 4 and 5). It was also indirectly confirmed by the changes in AI values as a function of size: larger MEPs (> 1.5 mm) were very transparent (mean 0.21, std 0.10) in the stratified layer compared to the other layers (mean 0.50, std 0.18; Fig. 6b).

(3) Situations without stratification and with high chl-*a* concentrations were associated with a low AI and a relatively low %MEPs (Figs 2 and 4). This situation is exemplified in the surface layer at station C, and to a lesser extent in the middle layer (40 to 75 m depth) at station A. It also corresponds roughly to all the stations within habitat #1, characterized by mixed waters and high chl-*a* concentrations (Fig. 2). In such situations, the peak in MEP size spectra appears to be shifted towards smaller size classes (Fig. 6a). Accordingly, MEP size in habitat #1 was generally much

smaller than in habitat #2 (high chl-*a* concentration and stratification), with an average of 505 µm ESD (406-705 µm) and 823 µm ESD (619-1387 µm), respectively.

(4) The AI stayed relatively constant over all the stations without stratification or high chl-*a* concentration with an average value of 0.25 (std 0.05).

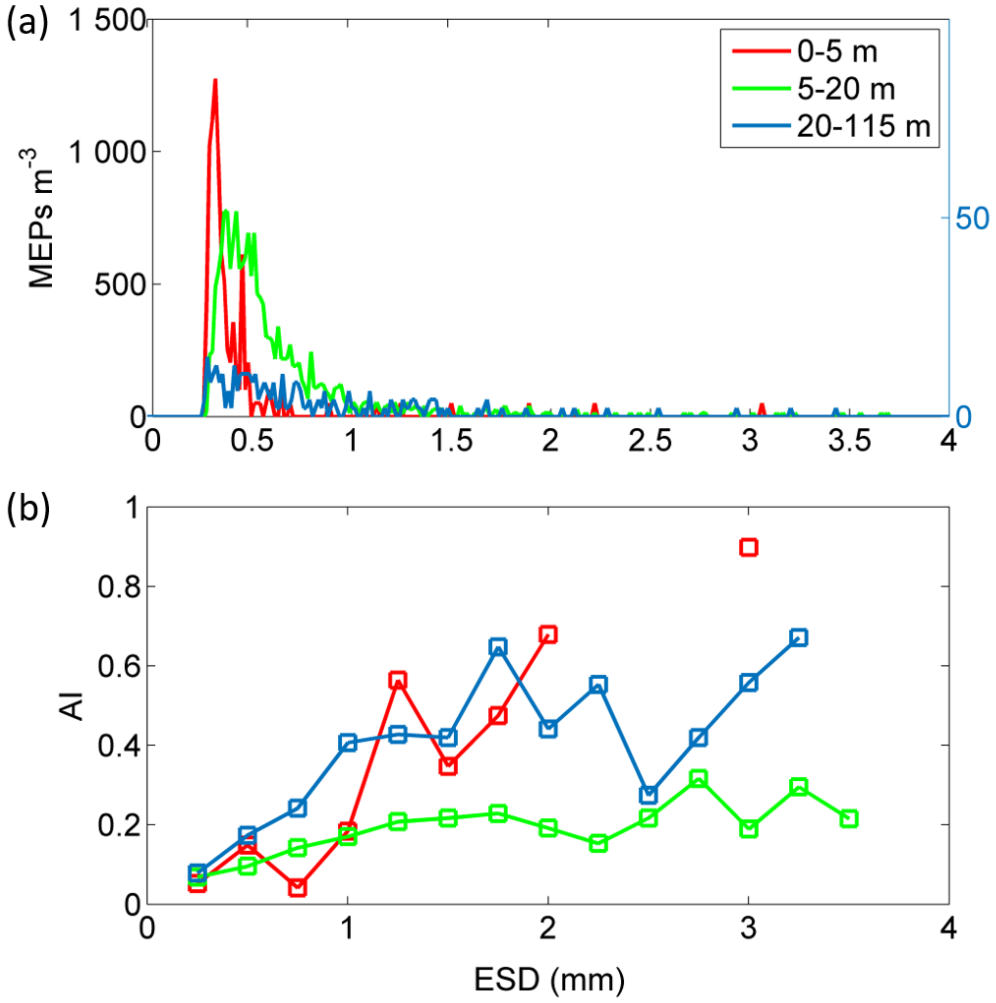

Fig. 6. (a) Size spectra of MEPs and (b) mean attenuance index (AI) as a function of the MEP size (0.1 mm interval) at station C (see Fig. 2, 4 & 5) in 3 different water layers. Because of lower values, MEP abundances for the deepest layer (20-115 m) is displayed on a separate axis (right).

4. Discussion

4.1. Optimal conditions to use the LOPC as a zooplankton counter

Based on our dataset from the coastal waters of the Northwestern Mediterranean Sea, we identified three main ecological situations where the LOPC counted various amounts of detritus. In unstratified water columns with low chl-*a* concentrations (< 1 mg m^{-3}), LOPC abundances were comparable to net abundances, meaning that the LOPC counted mostly zooplankton and only few detritus. This was reflected by LOPC particles having a low %MEPs in total counts (< 2 %), and a high mean AI (> 0.2). In stratified waters with high chl-*a* concentrations, LOPC abundances were up to ten times higher than net abundances most likely due to the LOPC counting detritus. In this situation, LOPC counts were characterized by high %MEPs and low AIs. In stratified waters with low chl-*a* concentrations, LOPC abundances were also higher than net abundances but in a lesser extent, and particles here were again characterized by a high %MEPs and a low AI. These results suggest that information on the large particles counted by the LOPC (MEPs) can be used to infer the percentage of detritus counted by the LOPC. Our results also suggest that the LOPC counted mainly living organisms when the %MEPs was < 2 %, a more conservative limit than the 5 % limit found by Schultes and Lopes (2009) off the Brazilian coast. In most water columns without stratification and/or high chl-*a* concentration the mean AI remained constant, around 0.25, which allowed us to define a threshold below which aggregation or phytoplankton chains likely occur. The usage of %MEPs and AI as indicators of different physical and biological situations is summarized in Table 3. By applying our thresholds to the data from our study area and to data from high latitudes, we could identify in total four different situations in which detritus represent between 0 and 90 % of the total LOPC counts.

Table 3. Summary describing how to interpret the LOPC abundance with the help of the two indicators, %MEPs and AI. The thresholds defined in this study lead to 4 situations. The possible causes for these situations are detailed and clues to interpret the data based on the study context are proposed. The threshold for overestimation (5 %) is from Schultes and Lopes 2009.

	Low AI (< 0.2)	High AI (> 0.2)
High % of MEPs (> 2) (> 5 overestimation)	Aggregate formation if stratified waters, can be promoted by high primary production in surface layer. Sediment input or resuspension in nearshore areas.	High concentration of big copepods (> 1.5 mm), mainly in high latitude areas, or terrestrial input (sand).
Low % of MEPs (< 2)	Low detritus abundance. If high chl-*a* concentration, phytoplankton chains or colonies characterized by small MEP size (< 400 µm ESD)	Clear water, LOPC mainly counting zooplankton.

4.2. Potential biases linked to the sampling protocol

The LOPC was placed on the CTD rosette to obtain simultaneous profiles of physical and biogeochemical parameters and net tows were conducted afterwards. The time lag between a LOPC cast and corresponding net tow could have affected the comparison between ZooScan and LOPC results, even though it was reduced to its minimum. The general patchiness of particles and zooplankton in the water column can create some variability in abundance data collected at the same location over a short amount of time. In general however, the vertical distributions of particles

measured by the LOPC along the coastal-offshore transects (stations separated by 5 km) showed consistent abundances between the stations with gradual changes, suggesting a limited patchiness. Furthermore, for the majority of the offshore stations with no stratification and low chl-*a* concentration, the percentage of detritus was intermediate and rather constant (mean 39, standard deviation 17). Therefore, we argue that even if patchiness potentially created some variability blurring our results, especially where percentage of detritus was low, at most of our stations it was valid to use a comparison of abundances to determine the detritus contribution. At 3 out of 78 stations, abundances determined from net samples were >30 % higher than those determined by the LOPC, two of these stations being in shallow waters. We suggest that these values might be due to technical issues (difference in sampling depth, mistake through the subsampling preparation, etc.) and they were, therefore, not included in any part of the analysis.

4.3. Impact of stratification and/or high production on LOPC counts and the formation of MEPs

The relationship between the detritus distribution and the habitats defined in E2014 (Table 2) provided a good base to analyze the link between detritus formation and environmental conditions. Consistent results were found analyzing the spatial distributions and the vertical profiles in the changes of percentage of detritus, LOPC counts and MEP characteristics. The stratification of the water column seems to be the main factor influencing the vertical distribution of LOPC counts. The interface between water layers of different densities acts as a barrier, locally accumulating particles. The high concentrations of particles within pycnoclines can be explained by the change in buoyancy of aggregates, reducing their downward settling velocities (Macintyre *et al.*, 1995, Prairie *et al.*, 2015). Our case study from the Mediterranean Sea shows that this process induces particle aggregations resulting in the formation of transparent MEPs with a low AI (< 0.2), and in

an increase of the %MEPs in total counts (see again Fig. 1, situation described in the upper left part of the Table 3). The mechanisms underlying the aggregate formation can be mechanical, due to transparent exopolymer particles, mucus or dead phytoplankton cells (Alldredge and Silver, 1988), or chemical, when strong salinity changes promotes flocculation processes. When such a stratification is combined with high production in the surface layer, the higher concentration of particles will promote the formation of more aggregates, resulting in very high %MEPs.

When high chl-*a* concentrations were not associated with stratification, the size of the MEPs was smaller and the AI decreased below 0.2 while the %MEPs remained constant. One explanation is that without stratification, settling particles could freely fall through the water column, and the probability of colliding between particles is reduced. But also, phytoplankton colonies typically produce small MEPs with lower AI due to a high degree of empty space at the activated photodiodes. Further investigations at stations that show a large contribution of detritus could also give insight into the changes of the size structure of organic matter in different water layers, which could be useful to study carbon vertical flux.

4.4. Limits of the methods

Our method is based on the information from the MEPs, which represent only a small part of the LOPC counts, but we successfully extrapolated this result to assess the contribution of detritus in the total LOPC counts. We suggest that there is a relationship between the % of SEPs being detritus and the %MEPs in LOPC counts. Indeed, the aggregation processes described earlier in the text (see 4.3) attest that if detritus represents a substantial part of the SEPs, some will aggregate and end up as MEPs. This is due to the detritus constitution and has been described by several studies focusing, for instance, on phytoplankton blooms (Alldredge and Jackson, 1995) or appendicularian houses (Lombard and Kiørboe, 2010).

In some specific cases the %MEPs can be affected by others causes than the ones described in this study. In places with very clear water and high concentrations of big organisms, e.g. *Calanus finmarchicus* overwintering in North Atlantic waters, the %MEPs can drastically rise even though the percentage of detritus is low (Table 3, upper right). In that case, we suggest to use the AI alone as an indicator to separate between living and non-living particles (Checkley et al*.,* 2008; Gaardsted et al*.,* 2010), and estimate the part of the MEPs being detrtital particles. In this study, where the dominating species were small copepods, we assume that MEPs that have a low AI were detritus. However, transparent gelatinous organisms can also a have similar MEP signal. Given the opening of the LOPC tunnel (7 x 7 cm), appendicularians are among potential organisms that can be counted by the LOPC in amounts high enough to affect the MEP signal. In our case, although substantial abundance of appendicularians were recorded during the winter cruise (ca 30 000 # m^{-2}), this did not seem to affect the MEP signal as the AI was higher in winter than during the spring cruise. Nevertheless, we suggest that when using the LOPC, occasional net samples are needed to describe the plankton community and to attest of peaks of specific groups such as gelatinous zooplankton.

4.5. Use of our results in other regions

The indicators developed in this study to interpret the detritus part of LOPC abundances are based on a large dataset collected in a coastal area of the NW Mediterranean Sea. However, the processes leading to the formation of detritus are not specific to this area. They take place in the epipelagic zone of most of the marine ecosystems, and it is likely that these indicators will be valid in other areas. To test this, we applied the thresholds for %MEPs and AI that were developed in this study to other datasets from around the globe.

A dataset collected in a tropical system (Schultes and Lopes, 2009), sampled from mixed and weakly stratified stations over the continental shelf and slope, had generally a low %MEPs (mean

0.87, standard deviation 0.33) and rather high AIs (mean 0.22, standard deviation 0.04) over 37 stations (Table 4). The biomass estimated with the LOPC for particles > 500 µm ESD was significantly correlated to zooplankton displacement volume of net samples (n= 37, r= 0.4, p< 0.01), indicating a limited influence of detritus (Table 3, lower right).

Two datasets from polar areas (Antarctic Peninsula and Svalbard) were characterized by clear water, and LOPC counts had a very low %MEPs (< 0.5 %) and generally high AIs (> 0.2). Here, the indicators show that the LOPC counted mainly zooplankton (Table 3, lower right), which was supported by a good agreement between LOPC and net data.

In an Arctic fjord characterized by glacial melt water input, freshwater run-off resulted in a dramatic increase in LOPC counts (> 500 x 10^3 # m^{-3}) in the inner part of the fjord and very low AI values in the entire fjord (Trudnowska et al., 2014). The %MEPs, on the other hand, was gradually decreasing from 3.90 in the inner part to 1.16 in the outer part while the zooplankton abundances estimated from net tows were rather constant along the transect. Based on the thresholds developed for the indicators %MEPs and AI, the fjord can be divided into two areas, i.e. the inner part characterized by high %MEPs, low AIs and high (glacial) detritus concentrations (Table 3, upper right); and the outer part characterized by low %MEPs, low AIs, high chl-*a* concentration and realistic zooplankton abundances estimated by the LOPC (Table 3, lower left).

Table 3. Comparison of particle characteristics in different regions and different environmental conditions. Only stations deeper than 50 m were included. High chl-*a*: max chl-*a* > 1 mg m^{-3}.

Environmental conditions	Region / remarks	# part m^{-3} min-max nbr. of stn.	AI mean (min-max)	%MEPs mean (min-max)	References
Mixed waters	Antarctic Peninsula – Continental bay Clear water and few large-sized organisms	3600 – 36200 *n=16*	0.24 (0.09 – 0.54)	0.34 (0.16 – 1.61)	Espinasse et al., 2012
	Svalbard – Cross shelf section	2000 – 26000 *n=10*	0.48 (0.36 – 0.56)	0.33 (0.14 – 2.17)	Basedow, Unpublished data
	North Atlantic – Open ocean Very clear water	4000 – 6000 *n=3*	0.46 (0.31 – 0.62)	0.76 (0.70 – 0.85)	Basedow et al., 2016
	Brazil coast – Continental slope	6900 – 146000 *n=37*	0.22 (0.13 – 0.3)	0.87 (0.54 – 2.04)	Schultes and Lopes, 2009
	NW Mediterranean Sea – Continental slope	18000 – 30000 *n=43*	0.25 (0.11 – 0.44)	0.90 (0.40 – 1.92)	This study
	Polar fjord – Outer part high chl-*a*	130000 – 240000 *n=2*	0.10* (0.08 – 0.11)	1.16 (0.71 – 1.61)	Trudnowska et al., 2014
Stratified waters	Polar fjord – Glacier area Input of particles from melt-water discharge	475000 – 865000 *n=4*	0.08* (0.07 – 0.08)	3.90* (2.27 – 6.25)	Trudnowska et al., 2014
	NW Mediterranean Sea - Continental shelf	48000 – 70000 *n=8*	0.15* (0.11 – 0.22)	2.08* (1.13– 4.01)	This study
Stratified waters + high chl-*a*	NW Mediterranean Sea - Freshwater run-off	100000 – 215000 *n=13*	0.12* (0.07 – 0.14)	3.21* (1.70 – 5.36)	This study

*data which are out of the optimal conditions for LOPC use (based on the thresholds defined in Table 2)

5. Conclusion

We defined thresholds for two indicators based on LOPC data, which allowed to quickly check the contribution of detritus to total LOPC counts. These indicators were developed based on an extensive dataset from the Gulf of Lion and showed to be successful in different marine biogeographical regions. Applying the indicators %MEPs and AI provides a good basis to assess the detrital part in LOPC counts. When the thresholds for %MEPs and AI indicate that the LOPC is not mainly counting zooplankton, data should be interpreted carefully with respect to environmental data and the zooplankton community. This is especially important in shallow coastal waters, and more generally in strongly stratified waters. Here, LOPC data and other laser-based sensors should always be interpreted in parallel with a complementary dataset providing an independent estimate of the zooplankton part in particle counts.

Acknowledgments

This study is a contribution to the MERMEX-MISTRALS-WP2 'Ecological Processes'. The research cruises and laboratory analysis were supported by the project ANR COSTAS (ANR-09-CESA-007-04), whereas optical sensors implemented and used during the cruises were funded by ANR FOCEA (ANR-09-CEXC-006-01). The postdoctoral fellowship of BE was funded in the frame of the ConocoPhillips *Calanus* project (NSBU-107021) lead by the research network ARCTOS. The authors are grateful to the crews of the R/V Tethys II and SAM-M I O platform for their operation at sea and acknowledge the support of SOLAS, LOIZ and IMBER programs. We appreciate constructive comments on the manuscript by two anonymous referees.

References

Alldredge, A., Gotschalk, C.C., 1988. In situ settling behavior of marine snow. *Limnology and Oceanography*, 33, 339-351.

Alldredge, A.L., Jackson, G.A., 1995. Preface: Aggregation in marine system. *Deep Sea Research Part II: Topical Studies in Oceanography*, 42, 1-7.

Basedow, S.L., de Silva, N.A.L., Bode, A., van Beusekorn, J., 2016. Trophic positions of mesozooplankton across the North Atlantic: estimates derived from biovolume spectrum theories and stable isotope analyses. *Journal of Plankton Research*, 38, 1364-1378.

Basedow, S.L., Tande, K.S., Norrbin, M.F., Kristiansen, S.A., 2013. Capturing quantitative zooplankton information in the sea: Performance test of laser optical plankton counter and video plankton recorder in a Calanus finmarchicus dominated summer situation. *Progress in Oceanography*, 108, 72-80.

Basedow, S.L., Zhou, M., Tande, K.S., 2014. Secondary production at the Polar Front, Barents Sea, August 2007. *Journal of Marine Systems*, 130, 147-159.

Benfield, M.C., Grosjean, P., Culverhouse, P.F., Irigoien, X., Sieracki, M.E., Lopez-Urrutia, A., Dam, H.G., Hu, Q., Davis, C.S., Hansen, A., Pilskaln, C.H., Riseman, E.M., Schultz, H., Utgoff, P.E., Gorsky, G., 2007. Research on automated plankton identification. *Oceanography*, 20, 172-187.

Breiman, L., 2001. Random forests. *Mach. Learn.*, 45, 5-32.

Checkley, D.M., Jr., Davis, R.E., Herman, A.W., Jackson, G.A., Beanlands, B., Regier, L.A., 2008. Assessing plankton and other particles in situ with the SOLOPC. *Limnology and Oceanography*, 53, 2123-2136.

Davies, E.J., Nimmo-Smith, W.A.M., Agrawal, Y.C., Souza, A.J., 2011. Scattering signatures of suspended particles: an integrated system for combining digital holography and laser diffraction. *Opt. Express*, 19, 25488-25499.

Espinasse, B., Carlotti, F., Zhou, M., Devenon, J., 2014. Defining zooplankton habitats in the Gulf of Lion (NW Mediterranean Sea) using size structure and environmental conditions. *Marine Ecology Progress Series*, 506, 31-46.

Espinasse, B., Zhou, M., Zhu, Y., Hazen, E., Friedlaender, A., Nowacek, D., Chu, D., Carlotti, F., 2012. Austral fall-winter transition of mesozooplankton assemblages and krill aggregations in an embayment west of the Antarctic Peninsula. *Marine Ecology Progress Series*, 452, 63-80.

Gaardsted, F., Tande, K.S., Basedow, S.L., 2010. Measuring copepod abundance in deep-water winter habitats in the NE Norwegian Sea: intercomparison of results from laser optical plankton counter and multinet. *Fisheries Oceanography*, 19, 480-492.

Gasparini, S., 2007. PLANKTON IDENTIFIER: a software for automatic recognition of planktonic organisms., http://www.obs-vlfr.fr/ ~gaspari/Plankton_Identifier/index.php.

Gaudy, R., Youssara, F., Diaz, F., Raimbault, P., 2003. Biomass, metabolism and nutrition of zooplankton in the Gulf of Lions (NW Mediterranean). *Oceanologica Acta*, 26, 357-372.

González-Quirós, R., Checkley, D.M., Jr., 2006. Occurrence of fragile particles inferred from optical plankton counters used in situ and to analyze net samples collected simultaneously. *J. Geophys. Res.*, 111, C05S06.

Gorsky, G., Ohman, M.D., Picheral, M., Gasparini, S., Stemmann, L., Romagnan, J.-B., Cawood, A., Pesant, S., García-Comas, C., Prejger, F., 2010. Digital zooplankton image analysis using the ZooScan integrated system. *Journal of Plankton Research*, 32, 285-303.

Herman, A.W., Beanlands, B., Phillips, E.F., 2004. The next generation of Optical Plankton Counter: the Laser-OPC. *Journal of Plankton Research*, 26, 1135-1145.

Herman, A.W., Harvey, M., 2006. Application of normalized biomass size spectra to laser optical plankton counter net intercomparisons of zooplankton distributions. *Journal of Geophysical Research*, 111, 1-9.

Lombard, F., Kiørboe, T., 2010. Marine snow originating from appendicularian houses: Age-dependent settling characteristics. *Deep Sea Research I*, 57, 1304-1313.

Ludwig, W., Dumont, E., Meybeck, M., Heussner, S., 2009. River discharges of water and nutrients to the Mediterranean and Black Sea: Major drivers for ecosystem changes during past and future decades? *Progress in Oceanography*, 80, 199-217.

MacIntyre, S., Alldredge, A.L., Gotschalk, C.C., 1995. Accumulation of Marine Snow at Density Discontinuities in the Water Column. *Limnology and Oceanography*, 40, 449-468.

Marcolin, C.d.R., Schultes, S., Jackson, G.A., Lopes, R.M., 2013. Plankton and seston size spectra estimated by the LOPC and ZooScan in the Abrolhos Bank ecosystem (SE Atlantic). *Continental Shelf Research*, 70, 74-87.

Marcolin, C.R., Lopes, R.M., Jackson, G.A., 2015. Estimating zooplankton vertical distribution from combined LOPC and ZooScan observations on the Brazilian Coast. *Marine Biology*, 162, 2171-2186.

Mermex group, 2011. Marine ecosystems responses to climatic and anthropogenic forcings in the Mediterranean. *Progress in Oceanography*, 91, 97–166.

Ohman, M.D., Powell, J.R., Picheral, M., Jensen, D.W., 2012. Mesozooplankton and particulate matter responses to a deep-water frontal system in the southern California Current System. *Journal of Plankton Research*, 34, 815-827.

Petrik, C.M., Jackson, G.A., Checkley Jr, D.M., 2013. Aggregates and their distributions determined from LOPC observations made using an autonomous profiling float. *Deep Sea Research Part I: Oceanographic Research Papers*, 74, 64-81.

Prairie, J.C., Ziervogel, K., Camassa, R., McLaughlin, R.M., White, B.L., Dewald, C., Arnosti, C., 2015. Delayed settling of marine snow: Effects of density gradient and particle properties and implications for carbon cycling. *Marine Chemistry*, 175, 28-38.

R Development Core Team, 2017. *R: A language and environment for statistical computing.* Vienne, Austria: R Foundation for Statistical Computing.

Rakotomalala, R., 2005. TANAGRA : un logiciel gratuit pour l'enseignement et la recherche. *In : Actes de EGC 2005*, 2, 697-702.

Rasband, W.S., 2005. ImageJ. US National Institutes of Health, Bethesda, MD.

Schultes, S., Lopes, R.M., 2009. Laser Optical Plankton Counter and Zooscan intercomparison in tropical and subtropical marine ecosystems. *Limnology and Oceanography: Methods*, 7, 771-784.

Schultes, S., Sourisseau, M., Le Masson, E., Lunven, M., Marié, L., 2013. Influence of physical forcing on mesozooplankton communities at the Ushant tidal front. *Journal of Marine Systems*, 109–110, Supplement, S191-S202.

Talapatra, S., Hong, J., McFarland, M., Nayak, A., Zhang, C., Katz, J., Sullivan, J., Twardowski, M., Rines, J., Donaghay, P., 2013. Characterization of biophysical interactions in the water column using in situ digital holography. *Marine Ecology Progress Series*, 473, 29-51.

Trudnowska, E., Basedow, S.L., Blachowiak-Samolyk, K., 2014. Mid-summer mesozooplankton biomass, its size distribution, and estimated production within a glacial Arctic fjord (Hornsund, Svalbard). *Journal of Marine Systems*, 137, 55-66.

Vandromme, P., Nogueira, E., Huret, M., Lopez, U., Aacute, González-Nuevo González, G., Sourisseau, M., Petitgas, P., 2014. Springtime zooplankton size structure over the continental shelf of the Bay of Biscay. *Ocean Science*, 10, 821-835.

Zhang, X., Roman, M., Sanford, A., Adolf, H., Lascara, C., Burgett, R., 2000. Can an optical plankton counter produce reasonable estimates of zooplankton abundance and biovolume in water with high detritus? *Journal of Plankton Research*, 22, 137-150.

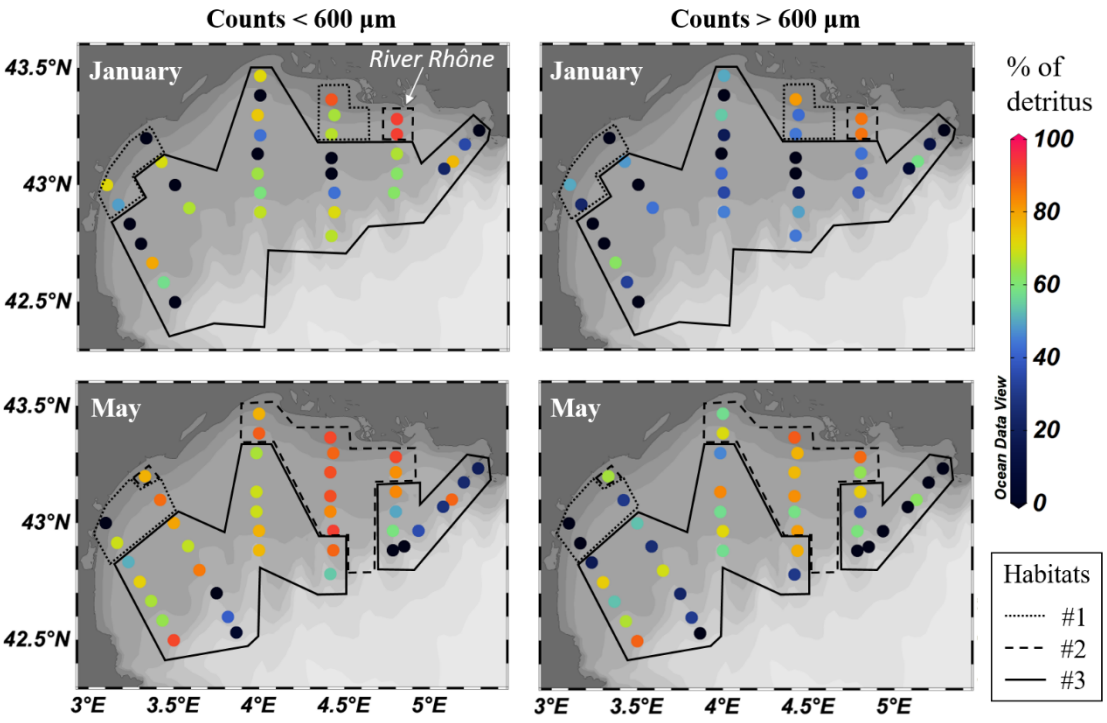

Fig. 1. Percentage of detritus in LOPC counts in January 2011 (top) and May 2010 (bottom) in the Gulf of Lion for two particle size fractions: below (left) and above (right) 600 µm size. The three habitats defined in Espinasse et al. 2014 are delineated, habitat #1: near shore area; habitat #2: area affected by the Rhône waters; habitat #3: continental shelf.

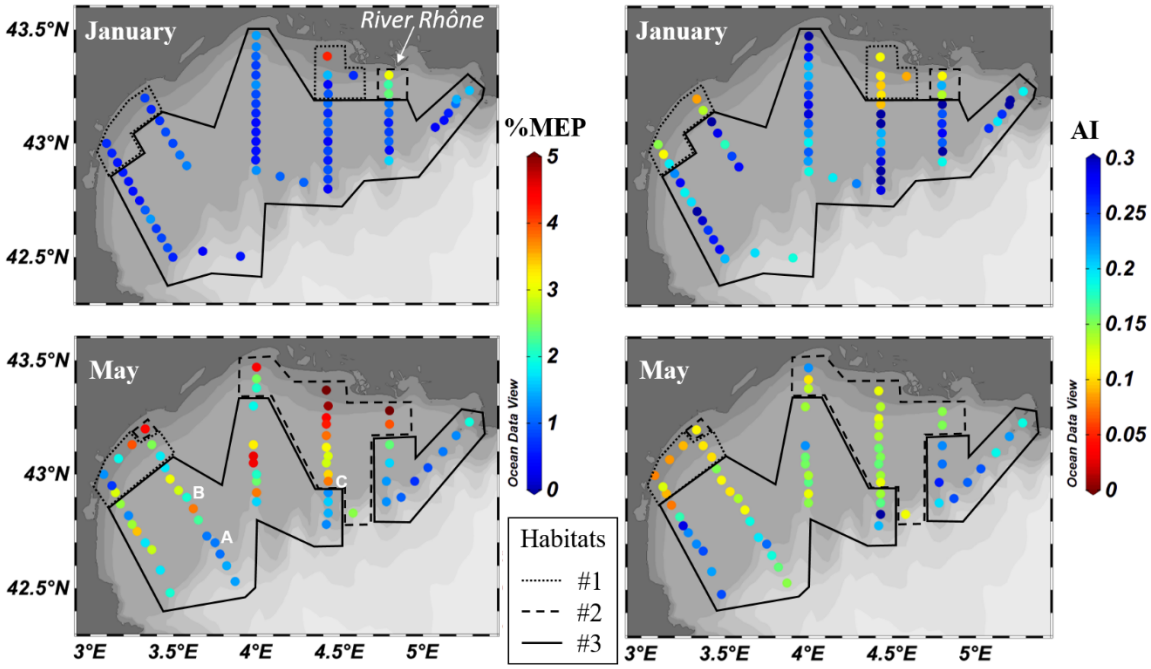

Fig. 2. Indicators of particles counted by the LOPC in January 2011 (top) and May 2010 (bottom) in the Gulf of Lion: % of MEPs in total LOPC counts (left side) and the MEPs' mean attenuance index (AI, right side). The three habitats defined in Espinasse et al. 2014 are delineated, habitat #1: near shore area; habitat #2: area affected by the Rhône waters; habitat #3: continental shelf. The three representative stations (A, B and C) shown in Fig. 4 are marked in the lower left panel.

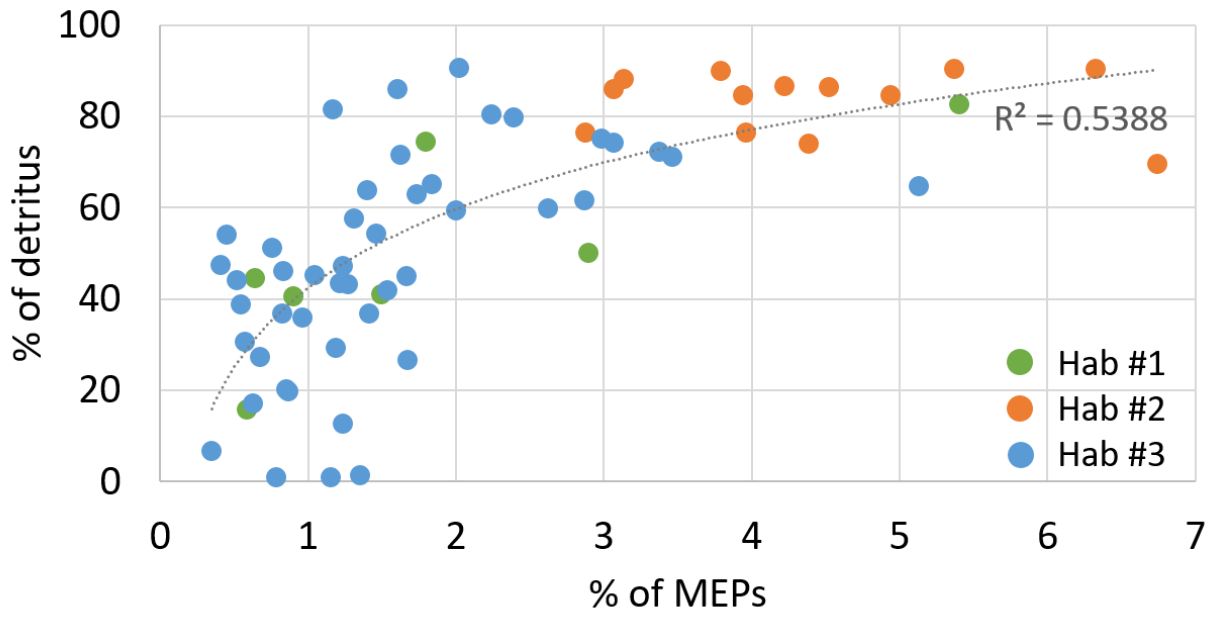

Fig. 3. Percentage of detritus in LOPC counts relative to the percentage of MEPs in total LOPC counts. The data were fitted with a logarithmic function. Habitats as defined in Fig. 1 and 2.

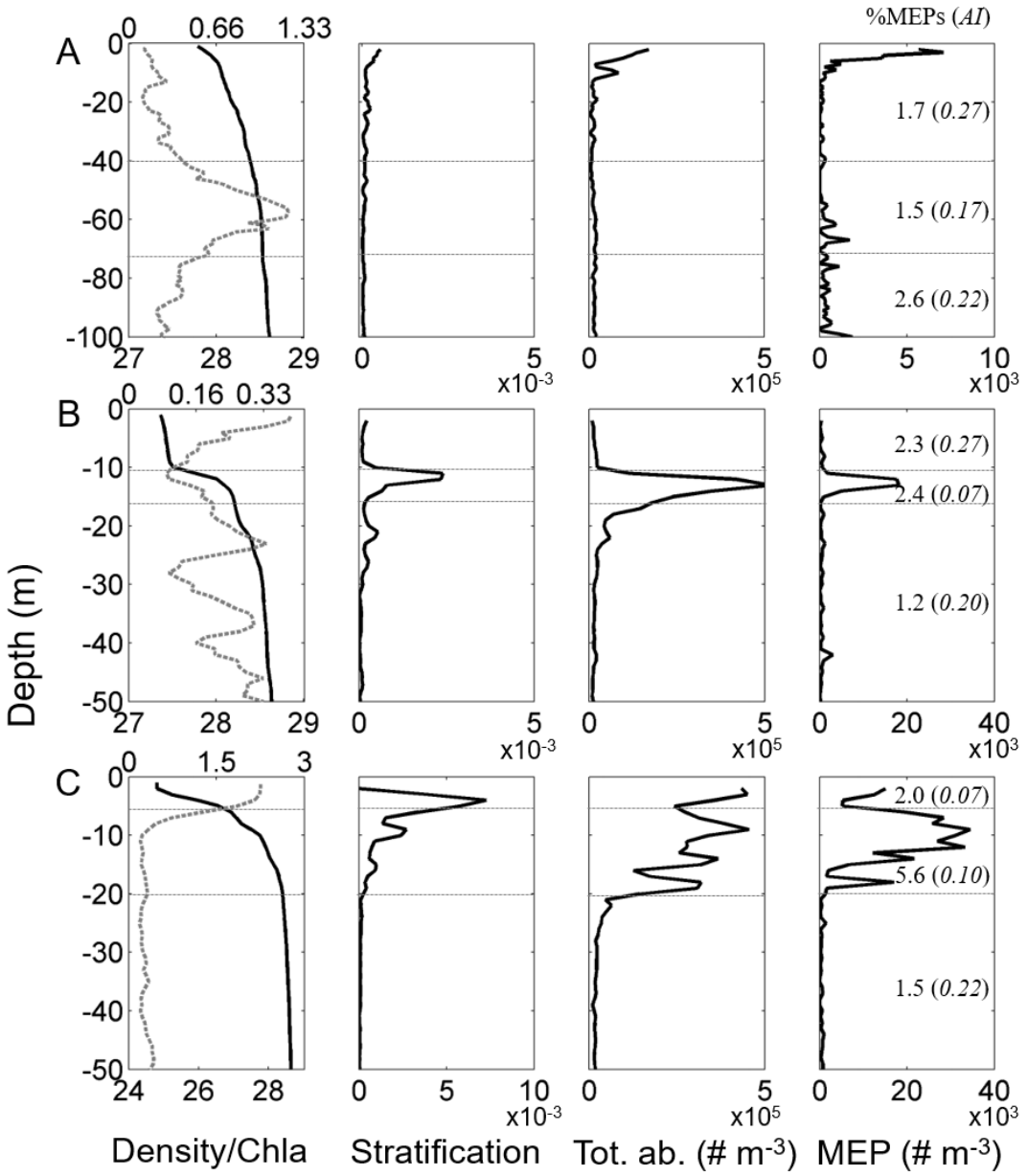

Fig. 4. Vertical profiles of water density σ_θ (kg m^{-3}; full line, left panels) and chl-a concentration (mg m^{-3}; dashed grey line, left panels), the stratification (Brunt-Väisälä frequency squared N^2, s^{-2} ; center left panels), total LOPC abundance (Tot. ab., centre right panels) and MEP abundance (right panels) at stations A, B and C typical of different environmental conditions. The integrated % of MEPs and the average of AI are specified in brackets for two (station A) or three (stations B and C) depth layers (horizontal dotted grey lines). The location of the stations is shown in Fig. 2. Note the change in x-axis range among stations.

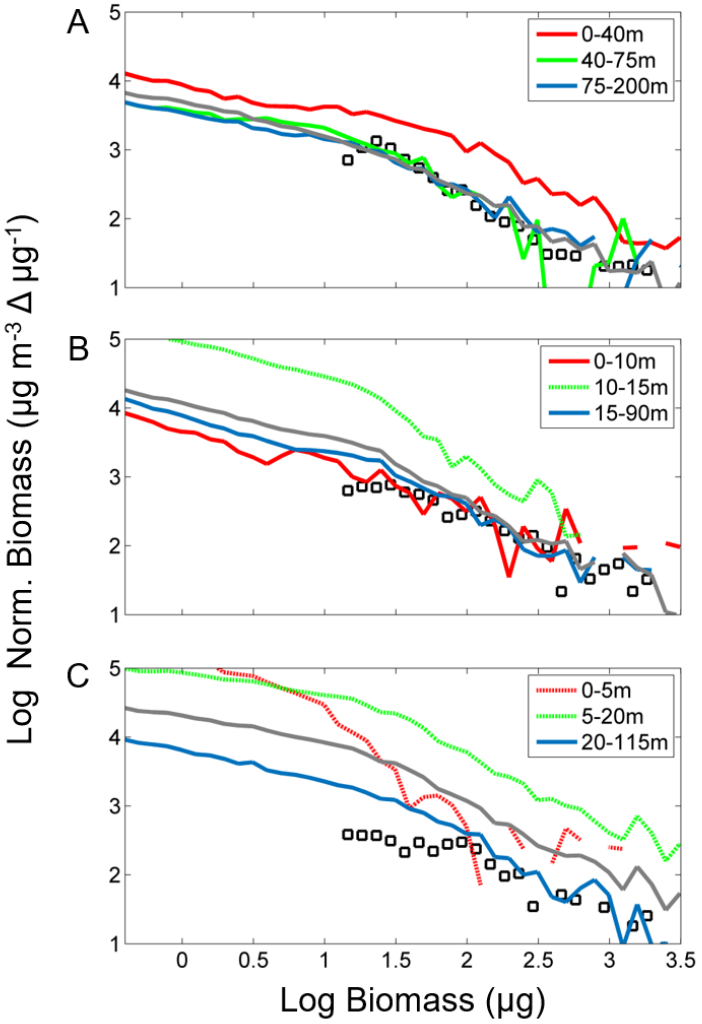

Fig. 5. Normalized biomass size spectra (NBSS) from LOPC data integrated over the water column (grey line) and in different layers as defined in Fig. 4 (blue lines, NBSSs in stratified layers are displayed with dashed line), and NBSS from ZooScan data over the whole water column (black squares) for 3 stations typical of different environmental conditions (see Fig. 2 and 4).

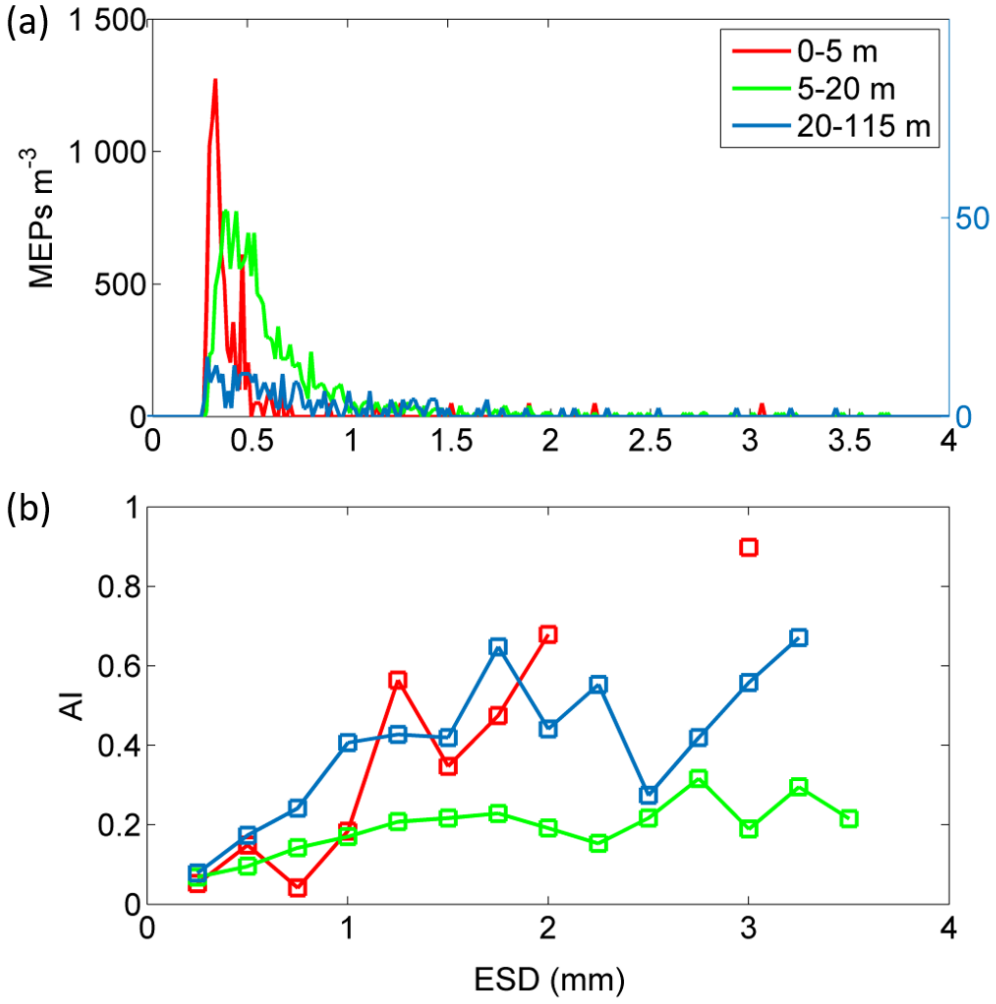

Fig. 6. (a) Size spectra of MEPs and (b) mean attenuance index (AI) as a function of the MEP size (0.1 mm interval) at station C (see Fig. 2, 4 & 5) in 3 different water layers. Because of lower values, MEP abundances for the deepest layer (20-115 m) is displayed on a separate axis (right).

Table 1. Station details including LOPC and ZooScan abundances (# part. m^{-3}), percentage of detritus in LOPC counts, percentage of MEPs in LOPC counts, mean AI, slope of the NBSS, water column stratification index, maximum of chl-*a* concentration (mg m^{-3}) and sampling depth. Considering the station denotation, the letter specifies the transect, from west (A) to east (F), and the number the position of the station along the transect from coast (1) to offshore (6-8). For example, A1 is the furthest west station and E1 is located in front of the mouth of the River Rhône. The stations A, B and C displayed in Figs 4-5 are indicated. No stratification is stated as n.a. for non-applicable. When ZooScan counts were higher than LOPC counts and, therefore, the percentage of detritus cannot be computed, x states for < 30 % difference in count and X > 30%.

Cruise	Station/ Habitat	LOPC Ab.	ZooScan Ab.	% of det.	%MEPs	AI	Slope	Strat. ind.	Max. chl-*a*	Depth
COSTEAU 6	A1/1	6514	3609	45	0.63	0.15	-1.07	n.a.	0.93	25
Jan 2011	A2/1	5427	4567	16	0.53	0.19	-0.96	n.a.	0.88	35
	A3/3	4533	5900	x	0.44	0.28	-0.87	n.a.	0.77	60
	A4/3	1955	3539	X	0.39	0.20	-0.99	n.a.	0.56	80
	A5/3	4370	1525	65	1.31	0.30	-0.73	n.a.	0.60	90
	A6/3	2426	1555	36	0.80	0.27	-0.81	n.a.	0.67	100
	A7/3	1815	1850	x	0.62	0.21	-0.94	n.a.	0.66	170
	B1/1	7111	21250	X	0.76	0.09	-1.30	n.a.	1.28	20
	B2/3	4046	1975	51	0.67	0.32	-0.79	n.a.	1.14	45
	B3/3	3005	3569	x	0.81	0.17	-0.93	0.03	0.97	80
	B4/3	3270	1853	43	1.19	0.28	-0.77	n.a.	0.82	90
	C1/3	9845	3567	64	1.37	0.39	-0.61	n.a.	0.83	20
	C2/3	6300	6985	x	1.00	0.27	-0.78	n.a.	0.92	45
	C3/3	2535	1364	46	0.78	0.21	-0.81	n.a.	0.52	75
	C4/3	3537	2500	29	0.89	0.26	-0.81	n.a.	0.77	80
	C5/3	2524	2903	x	0.62	0.29	-0.83	n.a.	0.70	85
	C6/3	2875	1605	44	0.47	0.22	-0.91	n.a.	0.63	90
	C7/3	1508	1048	31	0.45	0.24	-0.91	0.02	0.75	90
	C8/3	3856	2244	42	1.27	0.18	-0.86	n.a.	0.65	130
	D1/1	36498	6313	83	4.18	0.11	-0.77	0.67	1.40	17
	D2/1	4318	2543	41	1.49	0.11	-0.99	0.14	1.05	40
	D3/1	3209	1907	41	0.90	0.10	-1.14	0.25	0.99	65
	D4/3	2388	1979	17	0.63	0.42	-0.73	0.13	0.79	75
	D5/3	2834	3263	x	0.82	0.21	-0.88	n.a.	0.67	90
	D6/3	1548	1237	20	0.82	0.25	-0.79	n.a.	0.90	110
	D7/3	1756	803	54	0.89	0.31	-0.74	n.a.	0.45	270
	D8/3	453	238	48	0.33	0.29	-0.82	n.a.	0.46	200
	E1/2	10710	1500	86	3.06	0.11	-0.82	0.84	0.75	50
	E2/2	7154	965	87	2.35	0.14	-0.80	1.21	0.60	85
	E3/3	3065	1681	45	1.02	0.24	-0.80	0.20	0.74	95
	E4/3	2367	1495	37	0.80	0.28	-0.82	n.a.	0.71	100
	E5/3	992	608	39	0.43	0.32	-0.89	n.a.	0.53	300
	F1/3	3768	5250	x	1.56	0.19	-0.85	n.a.	0.71	55
	F2/3	2239	1641	27	1.11	0.38	-0.68	n.a.	0.70	80
	F3/3	1767	813	54	0.40	0.20	-0.84	n.a.	0.68	100

	F4/3	1257	1174	7	0.33	0.26	-0.95	n.a.	0.70	130
COSTEAU 4	A1/1	5924	9851	X	1.29	0.08	-1.02	0.06	1.70	25
May 2010	A2/1	15354	7646	50	2.90	0.09	-1.03	0.11	2.43	36
	A3/3	5343	3021	43	1.22	0.17	-0.89	0.05	0.87	55
	A4/3	4733	1361	71	3.46	0.23	-0.64	0.03	0.58	80
	A5/3	4168	1599	62	2.82	0.25	-0.66	0.03	0.63	80
	A6/3	3946	1462	63	1.73	0.22	-0.82	0.04	0.46	100
	A7/3	3088	287	91	2.00	0.25	-0.71	0.03	0.50	145
	B1/2	19440	5070	74	4.37	0.11	-0.79	0.29	0.33	20
	B2/1	10675	2725	74	1.78	0.10	-0.99	0.18	1.68	50
	B3/3	7298	1887	74	3.06	0.11	-0.87	0.20	0.73	80
Stn. B	B4/3	3933	1597	59	2.00	0.14	-0.78	0.17	0.53	90
	B5/3	2373	462	81	2.24	0.18	-0.74	0.11	0.82	150
Stn. A	B6/3	1687	1736	x	1.15	0.24	-0.80	0.04	1.10	200
	B7/3	2271	1433	37	1.41	0.16	-0.90	0.15	0.55	265
	B8/3	1411	1392	1	1.35	0.15	-0.92	0.10	0.76	200
	C1/2	44544	13513	70	4.44	0.22	-0.62	0.47	0.43	20
	C2/2	10514	1622	85	2.07	0.13	-0.87	0.28	1.35	45
	C3/3	5109	2046	60	1.89	0.14	-0.85	0.23	0.80	75
	C5/3	8609	2382	72	3.24	0.22	-0.65	0.25	0.90	90
	C6/3	8902	3134	65	4.50	0.15	-0.75	0.27	0.61	90
	C7/3	5193	1294	75	2.43	0.16	-0.76	0.36	0.91	85
	C8/3	3491	993	72	1.62	0.15	-0.85	0.24	0.41	140
	D1/2	33804	3244	90	5.87	0.12	-0.68	0.61	0.77	15
	D2/2	21171	3231	85	4.93	0.14	-0.62	0.41	0.69	40
	D3/2	16739	2239	87	4.22	0.13	-0.72	0.54	0.90	65
	D4/2	15823	1856	88	3.13	0.15	-0.71	0.74	1.20	75
	D5/2	11200	2645	76	2.87	0.16	-0.66	1.05	1.13	95
Stn. C	D6/2	8968	905	90	3.79	0.12	-0.68	0.51	2.27	115
	D7/3	4356	613	86	1.58	0.16	-0.89	0.40	0.49	200
	D8/3	1257	664	47	1.23	0.21	-0.79	0.25	0.59	200
	E1/2	40713	3925	90	5.21	0.15	-0.60	2.10	2.73	50
	E2/2	15312	3602	76	3.97	0.15	-0.72	0.71	2.70	90
	E3/3	10570	2130	80	2.38	0.23	-0.74	0.31	0.44	95
	E4/3	2734	1503	45	1.65	0.24	-0.74	0.07	0.54	100
	E5/3	2047	869	58	1.31	0.27	-0.76	0.06	0.49	200
	E6/3	2284	2922	x	1.29	0.20	-0.82	0.05	1.35	200
	F1/3	4991	5357	x	1.96	0.19	-0.79	0.02	0.73	60
	F2/3	2679	2340	13	1.22	0.22	-0.78	0.05	0.45	80
	F3/3	4086	755	82	1.15	0.19	-0.83	0.07	0.40	100
	F4/3	1816	1455	20	0.86	0.24	-0.83	0.03	0.54	200
	F5/3	1799	1307	27	0.67	0.24	-0.90	0.01	0.76	200
	F6/3	1645	2046	x	1.01	0.25	-0.83	0.02	0.55	200

Table 2. Kruskal-Wallis test applied on the percentage of detritus, % of MEPs and AI considering as factors the 3 habitats defined in Espinasse et al. 2014. Post-hoc results are also shown.

Parameter	X^2	p-value	Post-hoc			
%detritus	25.88	$2.39\ 10^{-6}$		Habitat #1	Habitat #2	H2 > H1;
			Habitat #2	<0.001	-	H2 > H3
			Habitat #3	n.s.	<0.001	
%MEPs	39.09	$3.23\ 10^{-9}$		Habitat #1	Habitat #2	H2 > H1;
			Habitat #2	<0.001	-	H2 > H3
			Habitat #3	n.s.	<0.001	
AI	61.85	$3.7\ 10^{-14}$		Habitat #1	Habitat #2	H3 > H1;
			Habitat #2	n.s.	-	H3 > H2
			Habitat #3	<0.001	<0.001	

Table 3. Summary describing how to interpret the LOPC abundance with the help of the two indicators, %MEPs and AI. The thresholds defined in this study lead to 4 situations. The possible causes for these situations are detailed and clues to interpret the data based on the study context are proposed. The threshold for overestimation (5 %) is from Schultes and Lopes 2009.

	Low AI (< 0.2)	High AI (> 0.2)
High % of MEPs (> 2) (> 5 overestimation)	Aggregate formation if stratified waters, can be promoted by high primary production in surface layer. Sediment input or resuspension in nearshore areas.	High concentration of big copepods (> 1.5 mm), mainly in high latitude areas, or terrestrial input (sand).
Low % of MEPs (< 2)	Low detritus abundance. If high chl-*a* concentration, phytoplankton chains or colonies characterized by small MEP size (< 400 μm ESD)	Clear water, LOPC mainly counting zooplankton.

Table 4. Comparison of particle characteristics in different regions and different environmental conditions. Only stations deeper than 50 m were included. High chl-a: max chl-a > 1 mg m^{-3}.

Environmental conditions	Region / remarks	# part m^{-3} min-max nbr. of stn.	AI mean (min-max)	%MEPs mean (min-max)	References
Mixed waters	Antarctic Peninsula – Continental bay Clear water and few large-sized organisms	3600 – 36200 *n=16*	0.24 (0.09 – 0.54)	0.34 (0.16 – 1.61)	Espinasse et al., 2012
	Svalbard – Cross shelf section	2000 – 26000 *n=10*	0.48 (0.36 – 0.56)	0.33 (0.14 – 2.17)	Basedow Unpublished data
	North Atlantic – Open ocean Very clear water	4000 – 6000 *n=3*	0.46 (0.31 – 0.62)	0.76 (0.70 – 0.85)	Basedow et al., 2016
	Brazil coast – Continental slope	6900 – 146000 *n=37*	0.22 (0.13 – 0.3)	0.87 (0.54 – 2.04)	Schultes and Lopes, 2009
	NW Mediterranean Sea – Continental slope	18000 – 30000 *n=43*	0.25 (0.11 – 0.44)	0.90 (0.40 – 1.92)	This study
	Polar fjord – Outer part high chl-a	130000 – 240000 *n=2*	0.10* (0.08 – 0.11)	1.16 (0.71 – 1.61)	Trudnowska et al., 2014
Stratified waters	Polar fjord – Glacier area Input of particles from melt-water discharge	475000 – 865000 *n=4*	0.08* (0.07 – 0.08)	3.90* (2.27 – 6.25)	Trudnowska et al., 2014
	NW Mediterranean Sea - Continental shelf	48000 – 70000 *n=8*	0.15* (0.11 – 0.22)	2.08* (1.13– 4.01)	This study
Stratified waters + high chl-a	NW Mediterranean Sea - Freshwater run-off	100000 – 215000 *n=13*	0.12* (0.07 – 0.14)	3.21* (1.70 – 5.36)	This study

*data which are out of the optimal conditions for LOPC use (based on the thresholds defined in Table 2)

Table S1. Mean values of the parameters within the 3 habitats for the two campaigns. Z_ML = Mixed layer depth, Rho_grad = Stratification index, Temp_0 = Sea surface temperature, Sal_0 = Sea surface salinity, Rho_b = Water density on the bottom, Chla_int = Integrated chl-*a* concentration, X0.1_0.3mm = Particle abundances from 0.1 to 0.3 mm ESD. From Espinasse et al, 2014.

	Z_ ML	**Rho grad**	**T_0**	**Sal_0**	**Rho_ b**	**Chla int**	**X0.1_ 0.3mm**	**X0.3_ 0.5mm**	**X0.5 mm**	**NBSS slope**
January										
Habitat #1	18	0.07	11.35	37.08	28.69	0.93	127910	6119	890	-1.15
Habitat #2	1	1.46	11.57	33.88	28.71	0.47	63480	7610	2730	-0.79
Habitat #3	74	0.02	12.58	37.70	28.70	0.53	35620	2932	1207	-0.85
May										
Habitat #1	1.8	0.13	16.16	36.78	28.72	0.50	165491	14800	3075	-1.03
Habitat #2	2.6	0.59	17.26	34.95	28.64	0.38	89478	15480	6389	-0.74
Habitat #3	5.3	0.13	16.19	37.07	28.73	0.32	31656	4698	1632	-0.80